RM E51J30

NACA RM E51J30

NACA
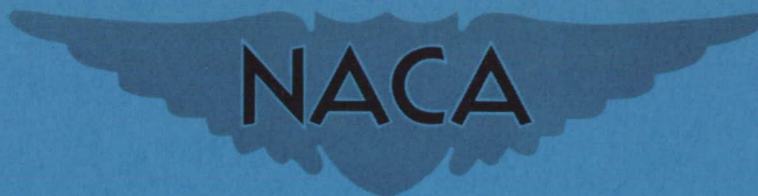
RESEARCH MEMORANDUM

PRELIMINARY INVESTIGATION OF CYCLIC DE-ICING OF AN AIRFOIL

USING AN EXTERNAL ELECTRIC HEATER

By James P. Lewis and Dean T. Bowden

Lewis Flight Propulsion Laboratory
Cleveland, Ohio

NATIONAL ADVISORY COMMITTEE
FOR AERONAUTICS

WASHINGTON

February 4, 1952

NATIONAL ADVISORY COMMITTEE FOR AERONAUTICS

RESEARCH MEMORANDUM

PRELIMINARY INVESTIGATION OF CYCLIC DE-ICING OF AN AIRFOIL USING

AN EXTERNAL ELECTRIC HEATER

By James P. Lewis and Dean T. Bowden

SUMMARY

An investigation was conducted in the NACA Lewis icing research tunnel to determine the characteristics and requirements of cyclic de-icing of a 65,2-216 airfoil by use of an external electric heater. The present investigation was limited to an airspeed of 175 miles per hour. Data are presented to show the effects of variations in heat-on and heat-off periods, ambient air temperature, liquid-water content, angle of attack, and heating distribution on the requirements for cyclic de-icing. The external heat flow at various icing and heating conditions is also presented.

A continuously heated parting strip at the airfoil leading edge was found necessary for quick, complete, and consistent ice removal. The cyclic power requirements were found to be primarily a function of the datum temperature and heat-on time, with the other operating and meteorological variables having a second-order effect. Short heat-on periods and high power densities resulted in the most efficient ice removal, the minimum energy input, and the minimum runback ice formations. The optimum chordwise heating distribution pattern was found to consist of a uniform distribution of cycled power density in the impingement region. Downstream of the impingement region the power density decreased to the limits of heating which, for the conditions investigated, extended from 5.7 percent chord on the upper surface of the airfoil to 8.9 percent chord on the lower surface. Ice removal did not take place at a heater surface temperature of 32° F; surface temperatures of approximately 50° to 100° F were required to effect removal. Better de-icing performance and greater energy savings would be possible with a heater having a higher thermal efficiency.

INTRODUCTION

The protection of aircraft in icing conditions can be achieved by continuously heating the critical components of the aircraft sufficiently to prevent the formation of ice. Past NACA research has

established the feasibility and the design basis for this system of anti-icing (references 1 to 3). An alternate thermal method of protection of aircraft in icing is the system of cyclic de-icing or intermittent heating. Recent design analyses (reference 4) have shown that the heat requirements for large high-speed, high-altitude aircraft using the method of ice prevention by continuous heating are extremely large and in some cases prohibitive. In addition, use of the hot-gas continuous anti-icing system, in the case of specific designs, may result in difficult design, structural, and installation problems. Preliminary analysis has indicated that the cyclic de-icing system possesses several advantages that would aid the solution of these protection problems.

Cyclic de-icing is that method of thermal icing protection in which ice is allowed to form for a relatively short period of time on the vulnerable component, and then heat is applied at a rate sufficient to melt quickly the bond of the ice to the surface, allowing aerodynamic or other forces to remove the ice. Upon ice removal, heating is terminated, allowing the surface to cool and re-ice, with the process being repeated in regular cycles. Since the heating is intermittent, heat can be supplied successively to small areas from a single source, thus reducing the heat-energy requirement over that required for continuous ice prevention. It would appear that a cyclic system can utilize several methods of heating, including hot gas and electric resistance heaters applied as either internal or external heaters. In particular, an electric cyclic de-icing system, in addition to reducing the heat-energy requirements over those for continuous heating, would have a generator weight of tolerable magnitude as compared with the prohibitive weight required for an electric anti-icing system operated continuously. A further possible advantage of the cyclic system is that such a system would tend to minimize the runback problem encountered with continuous heating when operating at an off-design condition.

Previous investigations of cyclic de-icing have been restricted to special cases, namely, the propeller (references 5 and 6) and jet-engine inlet guide vanes, and limited analytical studies (references 7 to 9). Application of the results of these investigations to airfoils is questionable for several reasons. In the case of propellers, centrifugal forces are present to aid removal of the ice. For an inlet guide vane, the size and shape of the vane and its attendant ice formation are considerably different from those of an airfoil of the size and shape generally employed in airplane wings and empennage. Limited experimental results of cyclic de-icing applied to airfoils have been reported by the National Research Council of Canada.

The analytical studies of the problem reported in references 8 and 9 employed an electric network analyzer in the solution of the transient heat flow. However, cyclic de-icing is a complex problem in transient

heat flow for which the boundary conditions are imperfectly known. These uncertain factors include the local heat-transfer coefficient and the local rate of ice accretion. More important the criterion of performance is as yet not specifically defined; that is, the point in time at which removal takes place is not given in independent terms to which the heat-transfer processes or the removal forces may be related. This is in contrast to the case of anti-icing for which there is the definite criterion of maintaining the surface at some specified temperature above freezing or evaporating certain amounts of water from the surface. Thus an analytical solution of the problem appears extremely difficult, and, in the absence of experimental data, would not necessarily be accurate or complete. For these reasons an experimental approach .was taken in the investigation of cyclic de-icing of airfoils in the NACA Lewis icing research tunnel.

The NACA is currently engaged in a general investigation of cyclic de-icing of airfoils including various types of heaters and methods of heating. The objectives of this investigation include a study of cyclic de-icing of airfoils to obtain a more complete understanding of the processes involved and to determine the criteria for successful operation of this method of ice protection. It is also desired to determined th' requirements for cyclic de-icing of airfoils in terms of the amounts of heat and cycle times required and to obtain the relation between these requirements and the meteorological and aircraft operatintgconditions.

In this report are presented the results of an initial phase of the investigation which employed an external electric heater of the rubber-clad type mounted on the forward portion of an 8-foot chord, 65,2-216 airfoil model in the NACA Lewis icing research tunnel. Preliminary studies and past experience with the cyclic de-icing of other bodies indicated that air speed is of second-order importance. For this reason, the present investigation was limited to an airspeed of 175 miles per hour. This restriction of airspeed permitted operation over a range of ambient air temperature, liquid-water content, angle of attack, and various heating configurations without damage to the experimental heaters from excessive heating. The drag penalties involved in cyclic de-icing are not reported. Continued investigations covering a full range of airspeed, determinations of the drag penalties, and studies of various types of heater are the subject of future research.

DESCRIPTION OF EQUIPMENT

The model used in the tunnel investigation of cyclic de-icing of airfoils consisted of a NACA 65,2-216 airfoil having an 8-foot chord and a 6-foot span mounted vertically in the test section of the 6- by

9-foot NACA Lewis icing research tunnel. An external electric heater
was installed on the forward portion of the airfoil. A photograph of
the airfoil model equipped with the heater installed in the tunnel is
shown in figure 1. The heater was centrally located spanwise and had
a length of 38 inches. The heater extended chordwise a surface distance
of 14.1 percent chord on the upper surface and 23.4 percent chord on the
lower surface. A sketch of the heater installation and details of con-
struction are shown in figure 2. The heater consisted of 1/8-inch-wide
Nichrome resistance strips each 0.001 inch thick spaced 1/32 inch apart
and running spanwise. The heater ribbons were enclosed between two
layers of glass cloth each 0.003 inch thick. The heater ribbons and
glass cloth were in turn sandwiched between two layers of neoprene. The
outer layer of neoprene was 0.012 inch thick and the inner layer between
the heater ribbons and the metal skin was 0.125 inch thick.

The heater was constructed on the leading-edge section of the air-
foil model with the successive layers cemented to each other to properly
locate and maintain the position of the thermocouples and heater ribbons.
The surface thermocouples were cemented to the outer layer of neoprene
and a thin coat of primer was then applied. Upon curing, the primer was
sanded smooth to expose the thermocouple junctions. The heater was
placed in an evacuated bag and then cured.

The heater ribbons were connected into several separate elements of
1/2, 1, and 2 inches in width which were distributed as shown in fig-
ure 2. Each element was connected to a separate variable autotrans-
former which permitted a selective control of the heat density and dis-
tribution in a chordwise direction. The heater elements were connected
to a variable cycle timer which permitted control of the heat-on and
heat-off periods. The total power input to each element was measured by
a recording wattmeter.

The ice formations on an airfoil ordinarily straddle the leading
edge in a glove-like manner, making it difficult for the external aero-
dynamic forces to effect removal of the ice. A continuously heated
strip near the stagnation point which would maintain an ice-free zone
has been proposed with the intention of facilitating removal by dividing
the ice cap into separate formations on the upper and lower surfaces.
Preliminary investigations have indicated improved de-icing by the use
of such a strip. For this reason manual by-pass switches that per-
mitted selected elements near the stagnation region to be heated either
cyclically or continuously at different power settings were installed
in the circuit. All elements that were cyclically heated were turned
on and off simultaneously.

The type of heater used in the investigation was based on a com-
promise of considerations of ease of construction and instrumentation,
the type of heater currently under consideration for actual installa-
tions, and the problem of control of the chordwise distribution of heat.

Numerous thermocouples were located in the central plane of the heater and were distributed in four layers as shown in figure 3. The two sets of thermocouples on each side of the heater ribbon enabled measurements to be made of the heat flow both inward and outward during steady-state conditions. The two outer layers of thermocouples were used in transient conditions to measure the heat flow outward from the heater to the ice. Calculations indicated that the thermal capacity of the outer layer of neoprene was small enough that the temperature gradient through the outer layer was essentially linear after approximately the first second of heating for the conditions of temperature and heat flux employed in the investigation. The thermocouples in the heater section consisted of 30 gage iron and constantan wire rolled down to a ribbon of approximately 0.0025 inch thickness. The ribbons were butt welded and were laid chordwise with the adjacent thermocouple junctions staggered to obtain the desired chordwise spacing. Thermocouples were also installed in the metal skin underneath and behind the heater. All thermocouples were recorded on flight recorders.

Measurement of the tunnel total temperature was obtained from shielded thermocouples located in the low-velocity section of the tunnel. All temperature measurements were referenced to a common bath temperature. The tunnel airspeed and angle of attack were obtained from the standard tunnel instrumentation. The liquid-water content and droplet size were obtained from a calibration of the tunnel spray system.

CONDITIONS AND PROCEDURE

Preliminary to the cyclic de-icing investigation, a determination was made with continuous heating in dry air of the effective thermal resistance of the layer of neoprene between the two outer layers of thermocouples. Measurements were made of the power input to each element and the temperatures throughout the heater. From the measured values of power and temperature an average effective thermal conductivity of 107.4 $Btu/(hr)(ft)^2(^\circ F)$ for the outer layer of neoprene was obtained. This value was used with the measured temperature drop obtained in subsequent cyclic de-icing tests to compute the heat flow from the heater to the ice. Within the accuracy of the temperature measurements it was not possible to find any variation of the conductivity with the mean temperature of the neoprene.

In the tunnel study of the requirements for cyclic de-icing the procedure was to determine by trial the minimum power density input and the chordwise distribution of heat for a specified heat-on period for given conditions of heat-off period, air temperature, airspeed, angle of attack, and water content. This optimum condition was defined as that power input that just resulted in complete and consistent ice removal at the end of the specified heat-on period. Upon attainment of

this optimum power input condition, all conditions were maintained constant and all pertinent data were recorded. Visual observations were made of the de-icing performance and photographs were taken during and after ice removal for each optimum set of conditions. Heat was applied to the wing before the sprays were turned on for most cases, but some runs were made with the heat applied after the water sprays were turned on.

The meteorological conditions investigated were as follows:

Liquid-water content (grams/cu m)	Volume median droplet size (microns)	Droplet size distribution[1]
0.25	6	D
.65	8	E
1.0	10	G

RESULTS

Continuously Heated Areas

Cyclic de-icing of an airfoil is much more difficult than that of a rotating body such as a propeller since centrifugal forces are not present to aid the aerodynamic forces in effecting ice removal. For this reason the use of the burn-through or parting strip has been proposed to facilitate ice removal. The parting strip consists of a narrow spanwise area located near the airfoil stagnation region and is continuously heated in contrast to the cyclic heating of the remaining heated area. The tunnel investigation included the use of the parting strip as well as runs with the entire area cyclically heated. Quick, complete, and consistent ice removal was accomplished only with the aid of the parting strip. For the case of all cycled heating, ice removal was obtained but it was sporadic; and good removal was usually obtained only on alternate cycles.

Parting-strip locations. - The location of the parting strip that resulted in the best ice removal is presented in figure 4 for various angles of attack. The heater-element arrangement around the leading edge and the location of the air stagnation point are also indicated.

---

[1]The droplet size distribution used herein is that defined in reference 10 and was obtained by the rotating multi-cylinder technique.

The best parting-strip location is very close to the stagnation point at each angle of attack. It might be assumed that the parting strip should be located at the point of the maximum rate of impingement to divide equally the formation. This point, as indicated by experience and the calculations of reference 11, lies between the stagnation point and the foremost point of the airfoil. The results of figure 4, however, indicate that the parting strip should lie between the stagnation point and the point of maximum impingement. For the full range of air temperature (19° to -11° F) it was necessary to use a parting strip 1 inch wide, as indicated in figure 4. At the higher temperatures (greater than 20° F) good removal was obtained with only a 1/2-inch strip. The precise location of the parting strip, however, was not found to be critical and variations in water content and droplet size had no appreciable effect. A single 1-inch-wide strip located at a point corresponding to elements 12 and 13 (fig. 4) would probably result in good removal over the full temperature range and a range of angle of attack of -2° to 6°.

Parting-strip temperatures. - Because of conduction losses to the adjacent cycled areas, a peak surface temperature of approximately 50° F was maintained at the center of the parting strip to insure a finite ice-free area and to prevent the adjacent ice formations from bridging over. The variation of the parting-strip surface temperature during de-icing is shown in figure 5(a) at various time intervals. The surface temperatures of the adjacent cyclically heated areas are also shown. For comparison the heated surface temperatures for the case in which all the heated elements including the parting strip area were cyclically heated is given in figure 5(b). All conditions of cycled power density, angle of attack, air temperature and speed, and liquid-water content were maintained constant for the two conditions. For the conditions of figure 5(a), a 1/2-inch-wide parting strip was used extending from 0.52 to 1.04 percent chord on the lower surface. The cycled power density used was the minimum required to obtain complete removal within the 30-second heat-on period. For the conditions of figure 5(b), the parting-strip area was cycled at the same power density as the adjacent cycled areas.

The results of figure 5(a) indicate an initial temperature peak in the parting-strip area which persists for approximately 5 to 10 seconds, at which time melting of the inner layer on the adjacent areas has begun. The peak temperature in the center of the parting strip exhibited very little change during the heating period, rising only 3° F, and during the heat-off period cooled to its initial temperature. The maximum variation in the peak parting-strip temperature was approximately 5° F. Comparing figures 5(a) and 5(b) shows that the direct effect of the parting strip on the adjacent surface temperatures is rather small, influencing only the area within approximately 0.5 percent chord on each side of the parting strip. The temperatures in the cycled areas

beyond the parting-strip area for the two conditions are very similar in
magnitude and rate of change. The results show a steady rise during
approximately the first 10 seconds of heating with sudden changes in
surface temperature occurring thereafter, together with large peak
values resulting on the lower surface. The greatest differences in the
surface temperatures occur near the leading edge where for the all-
cycled condition the curves become very irregular.

Parting-strip power requirements. - The input power densities for
the parting strip obtained in the tunnel investigation are shown in fig-
ure 6 as a function of the surface datum temperature. The determina-
tion of these power requirements was based on the criterion of the
minimum power required to maintain a finite ice-free area and the best
removal for a given condition. The surface datum temperature is defined
as the ambient air temperature plus the adiabatic rise, and in the case
of wet air conditions, minus the temperature depression resulting from
evaporation of water from the airfoil surface. The measured and cal-
culated dry datum temperatures agreed within the accuracy of the tem-
perature measurement. The wet datum temperature is an unheated hypo-
thetical temperature and cannot be measured during icing. For the range
of airspeed and temperature investigated, however, the difference in
the dry and wet datum temperatures is very small, being less than 3° F.
The power requirement was found to be essentially a single-valued func-
tion of the datum temperature with no significant variations resulting
from changes in angle of attack, water content, droplet size, or cycle
times.

A curve showing the net power to the outer surface as calculated
from the measured temperatures is also shown. The net power to the
outer surface is approximately 70 to 80 percent of the input power indi-
cating the efficiency of the heater. The calculated power required to
maintain the surface at 32° F is also shown in figure 6 as indicating
the minimum theoretical power requirement. This power was calculated
using the Martinelli equation (reference 12) for the heat-transfer
coefficient for the stagnation point of a cylinder and a water content
of 1.0 gram per cubic meter. These values differ from the measured net
powers primarily because of the higher temperatures (approximately 50° F)
used in the tunnel investigation.

Cyclically Heated Areas

As stated in the preceding section, prompt, complete, and consist-
ent de-icing was obtained only with the use of the parting strip. For
this reason the remainder of the discussion is concerned with the
results obtained from those investigations employing the parting strip
and necessarily includes data from the parting strip as well as from the

cyclically heated areas alone. The results are presented in terms of the cyclically heated surface temperatures, the chordwise distribution of the cyclic power, and the input and net cycled power requirements.

Surface temperatures. - Considerable uncertainty exists as to the thermal conditions occurring on the heater surface during de-icing, and especially as to those conditions required for ice removal. Some of the questions that arise in this connection concern: (1) the surface temperature required for ice removal, that is, whether removal takes place at 32° F; (2) the thickness of water film underneath the ice required for removal; (3) the effect of drainage of the melted ice inner layer; and (4) the relation between the surface temperature and the manner of ice removal. The experimentally determined surface temperatures provide a means of answering some of these questions and, in addition, provide values that may be used in checking a theoretical analysis of cyclic de-icing. Some indication of the surface temperatures existing in the cycled areas has been given in figure 5 in connection with the discussion of the parting strip. These temperatures are discussed in greater detail and their relation to the operating, heating, and meteorological variables and to the ice removal process is given.

In figure 7 a comparison is shown of typical measured heater surface temperatures at two locations (indicated by ratio of surface distance to chord length) on the airfoil in dry air and during cyclic de-icing. Both results were obtained at the same airspeed of 175 miles per hour, an angle of attack of 4°, and a tunnel total temperature of 20° F, which corresponds to a stagnation wet datum temperature of 19° F. The dry air time-temperature curves for the two locations shown in figure 7 are very similar with the temperature rise during the 15-second heating period being about the same. The initial dry temperatures are different because of the close proximity of the continuously heated parting strip to the 1.3 percent S/C location on the lower surface. The dry air temperature at 1.3 percent chord on the lower surface (fig. 7(a)) does not quite return to the initial value. This difference of 2° is attributed to inaccuracies in the temperature measurement. For both locations the initial temperature during de-icing is above the dry value because of the release of heat of fusion and the heat gain from the kinetic energy of the impinging water droplets. This rise is greater on the lower surface than on the upper surface in part because the local rate of impingement at an angle of attack of 4° is greater on the lower than the upper surface. The initial temperature on the lower surface is above freezing but observations showed ice present at this position. This ice was of a glaze slush-type formation and undoubtedly built up from formations on adjacent cold areas. The de-icing curve for the lower surface shows a break at about 9 seconds and thereafter increases rapidly in contrast to the upper surface, which maintains a smooth curve similar to the dry rise curve. This difference may have been caused by

the fact that very little ice formed on the upper surface and was quickly removed in one piece. On the lower surface the ice formation was larger and did not come off quickly but slid back slowly on the surface before being removed. The formation of wet slush ice, drainage of melted ice, formation of air pockets, and local roughness all affect the type of removal and give rise to discontinuities and irregularities in the heating curves. This break in the surface temperature-time curve was characteristic of slow and irregular ice removal and was usually associated with the longer heat-on periods.

A comparison of the surface temperature rise occurring during the heat-on period is shown in figure 8 as a function of the surface distance from the leading edge for dry air and during de-icing. For this particular condition, which is the same as that shown in figure 7, a 1/2-inch-wide parting strip near the stagnation point (approximately 3/4 percent chord on the lower surface) was used. The temperature rise rather than the actual surface temperatures is presented in this figure as being indicative of the changes in the heat flow during the cycled heat-on period and to permit a more direct comparison of points having different initial temperatures. The rise during de-icing is at every point less than that obtained in dry air with very little change in temperature occurring in the parting-strip area. Much greater differences in the wet and dry air rises were obtained on the lower surface than on the upper surface. Because of the higher ice collection rate on the lower surface, a greater insulating effect from the ice was obtained on the lower surface than on the upper surface; in addition, the slow, sliding type of ice removal on the lower surface contributed to the higher temperature rise obtained.

A comparison of typical surface heating and cooling curves during de-icing at various chordwise locations is shown in figure 9 for a condition of a datum temperature of 19° F, an angle of attack of 2°, and a water content of 0.65 gram per cubic meter. The heating times for this condition were 15 seconds on and 4 minutes off. The influence of the continuously heated parting strip on the adjacent areas is limited, extending only within 0.78 percent chord on the upper surface to 1.3 percent chord on the lower surface and appears almost solely as raising the initial temperature of the adjacent areas. All the heating curves are similar, and, as in the case of the curves of figure 7, the temperature rise upon application of the cycled heat is very fast with temperatures above 32° F being attained in less than 5 seconds. Greater variations exist in the cooling curves with the surface temperatures dropping below 32° F in less than 60 seconds except for those immediately adjacent to the parting strip.

A comparison of the time-temperature curves during de-icing at 2.34 percent chord on the lower surface is shown in figure 10 for three different heating times. These data are for a datum temperature of 19° F,

a water content of 0.65 gram per cubic meter, a heat-off time of
4 minutes, and an angle of attack of 2^O. The power input in each
case was the minimum required for complete removal to be achieved
within the specified heat-on period. This power requirement was
found to vary inversely with the heat-on time. The characteristic
break in the heating curve noted in figure 7(a) is again evident for
the 30-second heat-on condition. At this condition the ice removal
did not take place suddenly, but small pieces of ice were removed
over a relatively long period with sliding ice on the surface and
considerable drainage of melted ice. At the shorter heat-on periods
(and correspondingly higher power densities), the surface temperature
curves are smooth and reach higher peak values before removal of the
ice, as the heat-on time is reduced. The cooling curves are very
similar and the time required for the surface temperature to cool to
32° F varies from 21 to 23 seconds after the heat is turned off. The
total elapsed time in which the surface temperature is above 32° F is
32, 33, and 46 seconds for the 10, 15, and 30 second heat-on periods,
respectively. This is the maximum period in which runback of water can
occur. Thus it is advantageous to operate at the short heat-on conditions
to aid in reducing the amount of runback ice. An additional advantage
of the short heat-on periods is that less of the ice formation is melted
before removal occurs, thus further lessening the amount of runback.

Similar results are shown in figure 11 at a water content of 1.0
gram per cubic meter and a heat-off period of 2 minutes with all other
conditions the same. Because of the greater rate of accretion the
amount of ice collected is equal to or greater than that for the condi-
tions of figure 10, although the heat-off time is halved. Both the 15
and 30 second heat-on curves show a break and greater difficulty in
obtaining removal was experienced than for the 4 minute heat-off condi-
tion at the lower water content of 0.65 gram per cubic meter of fig-
ure 10. Also, the peak temperature for the 10-second heat-on condition
(fig. 11) is less than that for the longer heat-on time, which con-
trasts with the 4-minute heat-off results of figure 10 where an inverse
relation between peak temperature and heat-on time was obtained. No
direct explanation of these effects is apparent; the magnitude and
shape of the temperature rise is a complex function of the rate of ice
accretion, the amount of ice collected, the nature of the ice formation,
the adhesion of the ice to the surface, and the nature of the ice
removal as well as the rate of heat transfer and the aerodynamic removal
forces. The cooling curve for the 15-second heat-on condition shows a
dwell at about 30° F for a period of approximately 40 seconds. This
phenomenon was encountered several times and was of a random nature,
but was usually associated with the slower, more erratic type of ice
removal and the higher rates of ice accretion.

Typical surface temperature-time curves at this same location are shown in figure 12 at a datum temperature of -1° F for two heat-on times. In general the results are similar to those of figures 10 and 11, but much higher peak values were obtained. The higher peak temperatures are caused by the greatly increased power densities required at the low temperature condition for prompt removal.

Examination of the results of figures 7 to 12 shows that in no case did complete removal, which took place only at the end of the heat-on period, occur at a surface temperature of 32° F. The range of peak surface temperatures at which ice removal occurred extended from 50° to 100° F. Considerable variation in the surface temperature at the point of removal with the operating, meteorological, and heating conditions existed and no correlation of these results was possible. The point of ice removal cannot as yet be defined in terms of the surface temperature for specific conditions. The slower temperature rise curves as well as irregularities and breaks in the curves were found to be associated with the slower ice removal. A rapid and smooth rise in the surface temperature accompanied the fast removal obtained at the short heating periods as well as the minimum total time in which the surface temperatures were above the freezing point. At these short heating periods the ice removal occurred almost simultaneously at the end of the period, whereas with the longer heat-on, lower power density condition the ice was removed in numerous small pieces with the removal process taking place over a considerable portion of the heat-on period.

Distribution of cyclic power. - The construction of the experimental heater permitted the study of various chordwise distributions of the cycled heat. Thus it was possible to determine the optimum chordwise extent and distribution of heating for this particular type of heater. This optimum condition was defined as the minimum extent of heating and local heat input that resulted in the most complete and consistent ice removal together with the minimum amount of runback for a specific operating, meteorological, and cycle time condition. Typical optimum heating distributions are shown in figure 13 for two air temperatures and three heat-on times for an angle of attack of 2°. The location and relative magnitude of the parting-strip requirement are indicated. The power densities shown are the instantaneous densities based on the local areas heated at one particular time. With the exception of the continuously heated parting-strip area, an essentially uniform distribution of cycled power input in the region from approximately $1\frac{1}{2}$ percent chord on the upper surface to approximately $3\frac{1}{2}$ percent chord on the lower surface resulted in the best performance. This region of uniform power corresponded closely to the limits of direct water impingement. Downstream of this uniform area the power densities quickly reduce. Extending heating beyond the limits shown here did not aid in the de-icing nor in eliminating the amount of runback. The

extent of heating shown in figure 13 is that which provided good de-
icing over a range of angle of attack from 0° to 4°. Decreasing the
heat-on time resulted in an increase in the magnitude of the power
density requirement but caused very little change in the shape of the
distribution pattern except at the higher air temperature.

The variation in the heating distribution with angle of attack is
shown in figure 14. As might be expected the power on the upper surface
decreased with increasing angle of attack, with the opposite true on the
lower surface, for a larger percentage of the ice formation collected on
the lower surface as the angle of attack was increased.

Cycled power requirements. - The variation of the average input
cycled power density with datum temperature is shown in figure 15 for
various heat-on and heat-off times, liquid-water contents, and an angle
of attack of 2^O. The average of the cycled power densities between $1\frac{1}{2}$
percent chord on the upper surface and $3\frac{1}{2}$ percent chord on the lower
surface is taken as representative of the input cycled power density
requirement. For the range of conditions investigated, the power
density for a particular heat-on time appears to be primarily a function
of the datum temperature, with variation in the heat-off time and
liquid-water content having only a second-order effect. The power
density increases with decreasing datum temperature; the curves tend to
become linear at the lower temperatures. Higher power densities are
required with the shorter heat-on times, as was shown previously in
figure 13. This variation of power density with heat-on time may be
better shown by a cross plot of these data.

In figure 16 the power density is plotted against heat-on time for
a range of datum temperatures, two heat-off periods, and two liquid-
water contents. As shown in figure 16, the effect of heat-off period
and water content is small and is obscured by the scatter of the data.
The increase in power density with decreasing heat-on time is quite
rapid. Operation at heat-on times much less than 10 seconds would re-
quire a heater capable of withstanding very high power densities. At
the longer heat-on times the curves asymptotically approach finite values
of power density, and it would seem that operation at heat-on times in
excess of 40 seconds would not result in an appreciable reduction in
power density.

Practically no variation was obtained in the average input cycled
power density with angle of attack. The power density as a function of
angle of attack is shown in figure 17 for two datum temperatures and two
heat-off times at a constant heat-off time of 4 minutes. At a datum
temperature of 19° F the power density remains constant with angle of
attack. The power density for -1^O F shows a slight decrease with
increasing angle of attack. This effect may be caused by experimental
error, since it was difficult to determine precisely the exact point at
which the de-icing performance became marginal.

System Efficiency and De-Icing Effectiveness

The heat requirements for the cyclic and continuously heated areas have been presented separately. To evaluate the cyclic de-icing system consideration must be given to the combined heat requirements, a comparison of the cyclic requirements with those for ice prevention, the efficiency of the heater, and the effectiveness of the de-icing process itself, including the formation of runback ice.

Heater and system efficiency. - From the temperatures measured on the heater surface and those measured underneath the outer layer of rubber, the external heat flow from the heater surface during a cycle was calculated using the value of thermal conductivity determined in the dry air tests. A typical plot of this cumulative external heat flow during a complete cycle as a function of the cycle time is shown in figure 18 for a datum temperature of 19° F, a liquid-water content of 0.65 gram per cubic meter, an angle of attack of 2°, and a cycle of 15 seconds heat on and 4 minutes heat off. The heat flow is the cumulative heat dissipated from the heater surface integrated over the entire heated area and includes both the cyclic and continuously heated regions. Approximately 30 percent of the external heat flow is dissipated within the 15-second heating period. After the cyclic heat ceases the curve continues to increase fairly rapidly as the residual heat stored in the heater during the heat-on period is given up. Approximately 1 minute after the cyclic heating ceases the curve becomes essentially linear, the cyclic heat having been dissipated, and the only heat flow is that from the continuously heated parting strip. Similar results were obtained at the other operating, meteorological, and heating conditions with the percentage of the external heat flow during the heat-on period varying from approximately 30 to 65 percent of the total external heat flow for a complete cycle, and the larger values obtained at the longer heating periods.

A typical comparison of the cumulative external heat flow during a complete cycle with the total heat input is shown in figure 19 as a function of the chordwise surface distance. These results are for the same condition as figure 18. The large peak in the input and external flow curves at 0.26 percent chord on the lower surface is caused by the continuously heated parting strip. For the condition of figure 19, the integrated external heat flow is approximately 65 percent of the total input per cycle. For all conditions this efficiency ranged from approximately 60 to 80 percent. These efficiencies are indicative of the heat lost through the inner layer of neoprene to the unheated portions of the heater and the wing structure. The actual heat useful in de-icing is the total external heat flow during the heat-on period. Thus the true efficiency of the heater is the ratio of the total external heat flow during the heat-on period to the total energy input per cycle, and for the conditions of figures 18 and 19 this true efficiency would be 30 percent of 65 percent, or 19.5 percent.

The cumulative external heat flow during the heat-on period is plotted in figure 20 as a function of the heat-on time at a datum temperature of 19° F for two heat-off periods and two liquid-water contents. The data indicate a linear increase of the external heat flow with an increasing heat-on time as contrasted with the decrease in cycled input specific power density as indicated in figure 16. Insufficient data are available for a complete correlation of the effect of heat-off time and liquid-water content on the external heat flow. The results of figure 20(a), however, indicate that the external heat flow is not a direct function of ice thickness alone. The amount of ice collected is the product of the airspeed, time, liquid-water content, and collection efficiency. For a specific airfoil and fixed airspeed, altitude, and air temperature, a linear relation of collection efficiency to droplet size may be assumed. Thus the amount of ice collected for the 0.65 gram per cubic meter and 4 minute heat-off condition is equal to or slightly greater than the 1.0 gram per cubic meter and 2 minute heat-off condition. For this reason the differences in the heat flow for the two conditions cannot be explained on the basis of the insulating effect of the ice formation. The larger heat flow at the 1.0 gram per cubic meter and 2 minute heat-off condition may be explained by the greater rate of ice accretion rather than differences in ice thickness. The ratio of the cumulative external heat flow to the heat input during the heat-on period is shown in figure 20(b) with the same trends evident. For the heat-on conditions investigated, the external heat flow is one half or less of the input including both the cycled and continuously heated areas. For the very short heat-on periods, particularly less than 8 seconds, very low heater efficiencies are obtained and very little increase in efficiency would be obtained by operating at longer heat-on periods than those shown. More efficient utilization of the heat input would require a decrease in the heat capacity, an increase in the thermal insulation of the inner layer, and a decrease in the thermal resistance of the outer layer over the heating elements.

The results presented thus far have indicated low heater efficiencies and large cycled power density requirements for short heat-on conditions. Consideration must be given, however, to the system efficiency and the load on the heat source. For a practical installation the heater for a given aircraft or component may consist of several segments of equal area, each heated in turn, so that there would be no time in which an area is not being heated, with the resultant demand on the heat source being constant. For such a condition an equivalent continuous power density may be defined as the sum of the cycled power to an individual area at any one time and the total power to all the continuously heated areas divided by the total heated area of the aircraft or component. This equivalent continuous power represents the load on the heat source and is a correct measure of the cyclic system efficiency in terms of energy requirement. The equivalent continuous power

density is plotted in figure 21 as a function of the cycle ratio for two
datum temperatures and two liquid-water contents for an angle of attack
of 2°. The cycle ratio is defined as the time for a complete cycle di-
vided by the heat-on time. The curves show a sharp increase in equiva-
lent continuous power at the smaller cycle ratios where they approach a
cycle ratio of 1, or a condition of continuous heating. At the larger
values of cycle ratio the curves become asymptotic to a finite value of
power density equal to the parting-strip input divided by the total area
which is independent of the cycle ratio. This limiting parting-strip
requirement is indicated in figure 21 for each of the datum temperature
conditions. It is apparent that little gain in power saving is made by
the use of larger cycle ratios than those shown. For an actual system
the determination of the cycle ratio will depend not only on this con-
sideration of minimizing the energy demand on the heat source but also
on the number of segments into which the heated area may be divided
practically, together with the tolerance of the wing to the ice col-
lected during the off period in terms of aerodynamic penalties.

De-icing effectiveness and formation of runback. - The de-icing
effectiveness of the cyclic de-icing system may be measured by the
speed, completeness, and consistency of removal and the amount of run-
back ice formed together with the aerodynamic penalties incurred by the
direct impingement and runback ice formations. In the absence of meas-
urements of drag and other aerodynamic penalties, the system de-icing
effectiveness may be indicated by photographs taken during the de-icing
process. Typical de-icing and growth of the runback formation are shown
in figure 22. The pictures were taken during cyclic operation through
transparent sections in the tunnel side walls and show the lower surface
on the airfoil with the limit of heating indicated.

The ice formation after 8 minutes and 20 seconds, or just before
the second heat-on period, is illustrated in figure 22(a). The main ice
formation is shown and very slight amounts of runback ice may be seen on
the unheated portion of the heater. The next picture, figure 22(b),
taken after the third heat-on period, shows the removal of the main ice
formation and a slight increase in runback ice. Figure 22(c), taken
just before the ninth heat-on period, shows that the runback formation
has increased in size although very little in extent. The frost forma-
tions that have started to form downstream of the heated area are typi-
cal of those obtained in all tests and appear to be inherent to tunnel
operation. These frost formations increased in size and extent with
increasing amounts of runback and residual ice. A small amount of ice
downstream of the leading edge within the heated area is visible in
figure 22(d), taken at the end of the tenth heat-on period. This forma-
tion is apparent at the end of each heat-on period, but does not
increase in size and, consequently, may not be detrimental. The ice
formation prior to the twelfth heat-on period is shown in figure 22(e).

Figure 22(f) was taken after the thirteenth heat-on period, a total icing time of 56 minutes and 20 seconds. The residual ice formation is slight and the runback formation, although it has built forward on the heated area, is still small. Similar results were obtained on the upper surface of the airfoil. For the results shown in figure 22 the heat was applied to the parting strip before the water sprays were turned on. Other runs were made in which the heat to the parting strip was not applied until after the sprays were on for a full heat-off period. In this case removal was not obtained until the second heat-on period, but good de-icing performance was obtained thereafter.

The de-icing effectiveness shown in figure 22 was typical of that obtained at all conditions. The longer heat-on periods did not, as a rule, give the complete and consistent removal associated with the short heat-on, high power density heating cycles. The amount of runback was also observed to decrease with decreasing heat-on time. The chordwise location of the runback formation varied with the chordwise extent of heating; however, the size of the formation did not reduce materially with extended chordwise heating.

SUMMARY OF RESULTS AND CONCLUSIONS

For the range of variables investigated, the following results and conclusions may be stated:

1. A continuously heated parting strip in conjunction with cyclic heating was found necessary to insure quick, complete, and consistent ice removal. A 1-inch-wide continuously heated strip at the leading edge was sufficient for the range of datum temperatures from 19° to -11° F.

2. The most important variables in determining the cyclic power requirements are the datum temperature and the heat-on time; the heat-off time, the liquid-water content, and the droplet size have a second-order effect, and the angle of attack has no appreciable effect.

3. For the most efficient removal of ice, minimum runback ice, and minimum total energy input, the condition of high local power density and short (less than 15 seconds) heating period gave the best results.

4. The optimum cycled heat input distribution pattern consisted of a uniform power density for the region of water impingement. Extensive heating beyond the impingement region did not aid materially in de-icing performance or in eliminating runback ice.

5. The experimental heater was found to have a rather low thermal efficiency. Better de-icing performance and further economies in the

energy requirement would be obtained using a heater having a lower thermal capacity and a smaller thermal resistance between the heater elements and the outer surface.

6. Ice removal did not take place on attainment of a heater surface temperature of 32° F. For complete ice removal, peak surface temperatures of approximately 50° to 100° F resulted with a finite but undetermined water film formed underneath the ice formation.

Lewis Flight Propulsion Laboratory
    National Advisory Committee for Aeronautics
        Cleveland, Ohio

REFERENCES

1. Jones, Alun R., and Rodert, Lewis A.: Development of Thermal Ice-Prevention Equipment for the B-24D Airplane. NACA ACR Feb. 1943.

2. Neel, Carr B., Jr., Bergrun, Norman R., Jukoff, David, and Schlaff, Bernard A.: The Calculation of the Heat Required for Wing Thermal Ice Prevention in Specified Icing Conditions. NACA TN 1472, 1947.

3. Gelder, Thomas F., and Lewis, James P.: Comparison of Heat Transfer from Airfoil in Natural and Simulated Icing Conditions. NACA TN 2480, 1951.

4. Hacker, P. T., Dorsch, R. G., Gelder, T. F., Lewis J. P., Chandler, H. C., Jr., and Koutz, S. L.: Ice Protection for Turbojet Transport Airplane. S.M.F. Fund Paper No. FF-1, Presented at I.A.S. Fifth Annual Flight Propulsion Meeting, March 24, 1950.

5. Lewis, James P.: De-Icing Effectiveness of External Electric Heaters for Propeller Blades. NACA TN 1520, 1948.

6. Lewis, James P., and Stevens, Howard C., Jr.: Icing and De-Icing of a Propeller with Internal Blade Heaters. NACA TN 1691, 1948.

7. Scherrer, Richard: An Analytical Investigation of Thermal-Electric
      Means of Preventing Ice Formations on a Propeller Blade. NACA ACR
      4H31, 1944.

8. Tribus, Myron: Intermittent Heating for Aircraft Ice Protection
      with Application to Propellers and Jet Engines. Aircraft Gas Tur-
      bine Divs., Gen. Elec. Co. (Lynn, Mass.), Sept. 1949.

9. Weiner, Frederick R.: Further Remarks on Intermittent Heating for
      Aircraft Ice Protection. Paper No. 51-SA-38, A.S.M.E. Semi-Annual
      Meeting (Toronto), June 11-14, 1951.

10. Langmuir, Irving, and Blodgett, Katherine B.: A Mathematical
      Investigation of Water Droplet Trajectories. Tech. Rep. No. 5418,
      Air Material Command, AAF, Feb. 19, 1946. (Contract No. W-33-
      038-ac-9151 with Gen. Elec. Co.)

11. Guibert, A. G., Janssen, E., and Robbins, W. M.: Determination of
      Rate, Area, and Distribution of Impingement of Waterdrops on
      Various Airfoils from Trajectories Obtained on the Differential
      Analyzer. NACA RM 9A05, 1949.

12. Boelter, L. M. K., Grossman, L. M., Martinelli, R. C., and Morrin,
      E. H.: An Investigation of Aircraft Heaters. XXIX - Comparison
      of Several Methods of Calculating Heat Losses from Airfoils.
      NACA TN 1453, 1948.
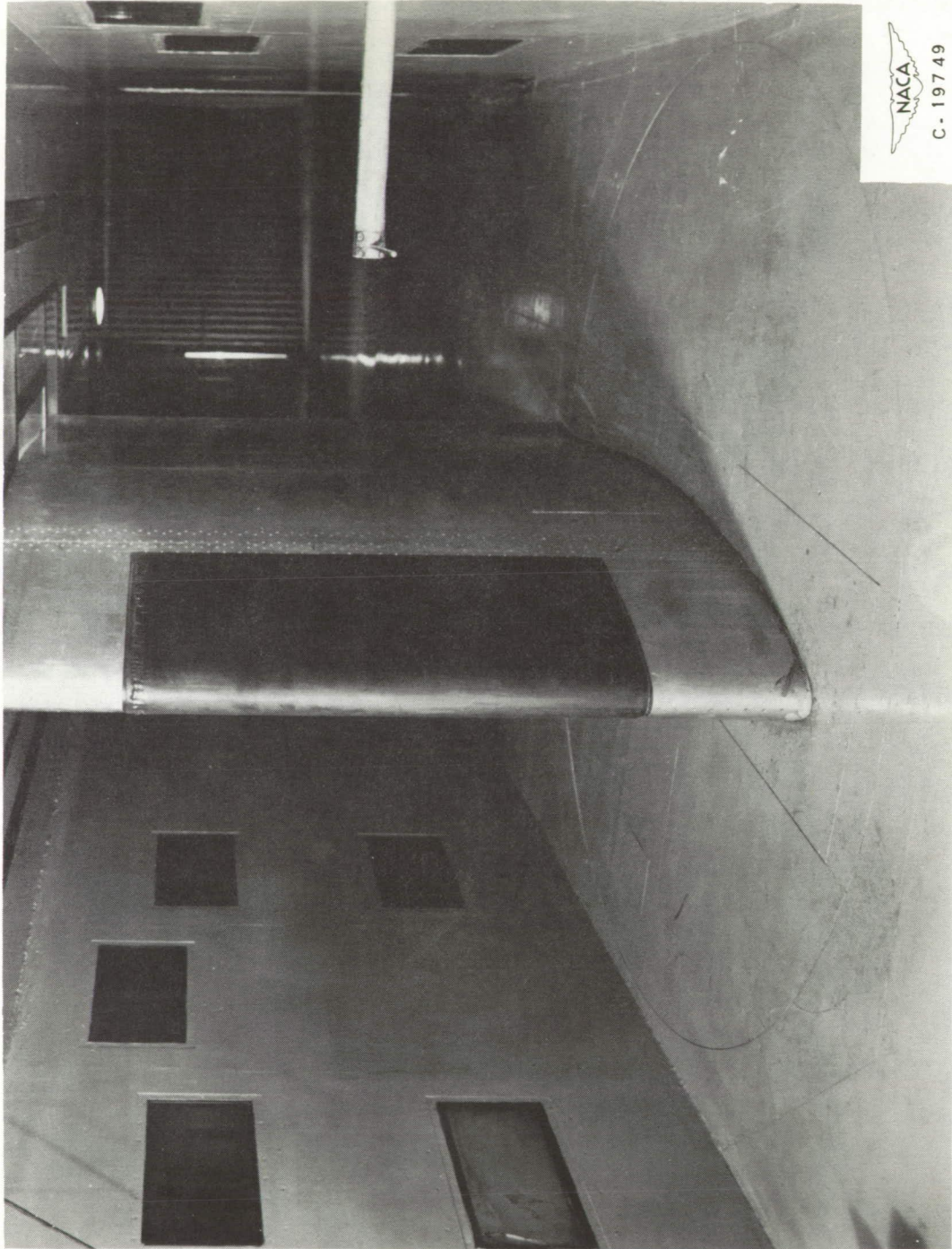
Figure 1. - Installation of airfoil model and heater in icing research tunnel.
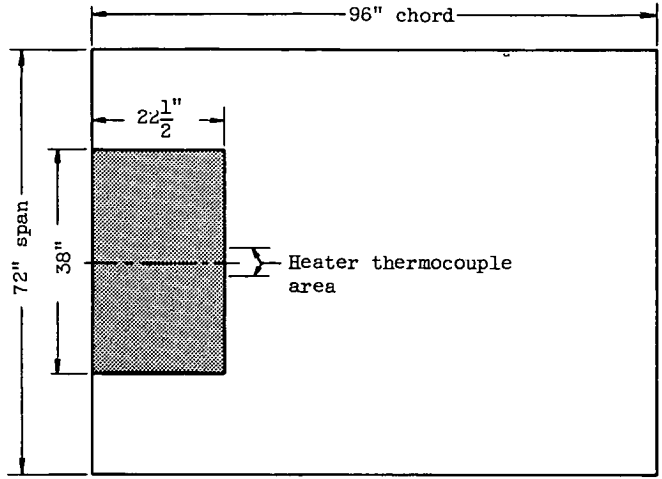
(a) Position of heater on lower surface of airfoil.
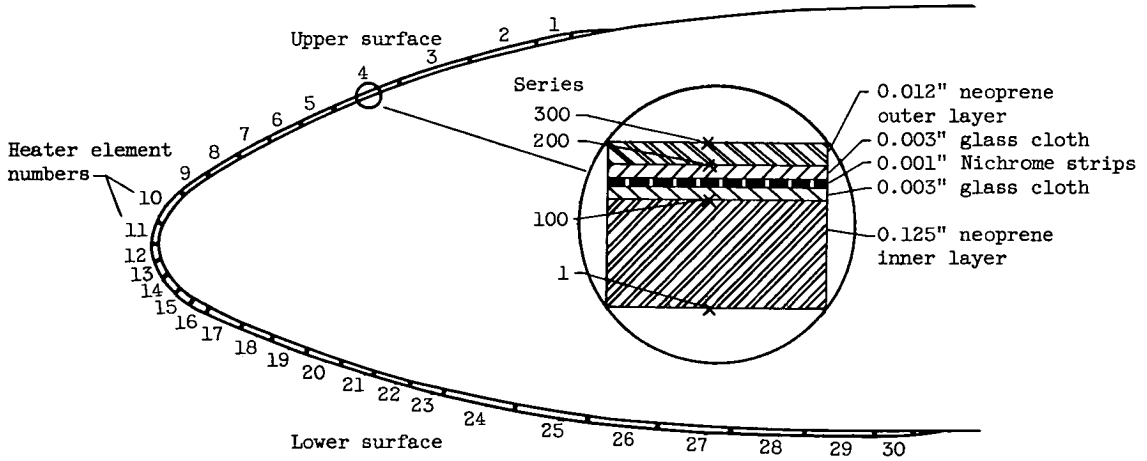
(b) Location of heater elements and details of heater construction.

Figure 2. - Heater installation and construction details.

Series

0.012" neoprene outer layer

0.125" neoprene inner layer

0.125" aluminum skin

300
200
100
1

Upper surface

Lower surface

NACA
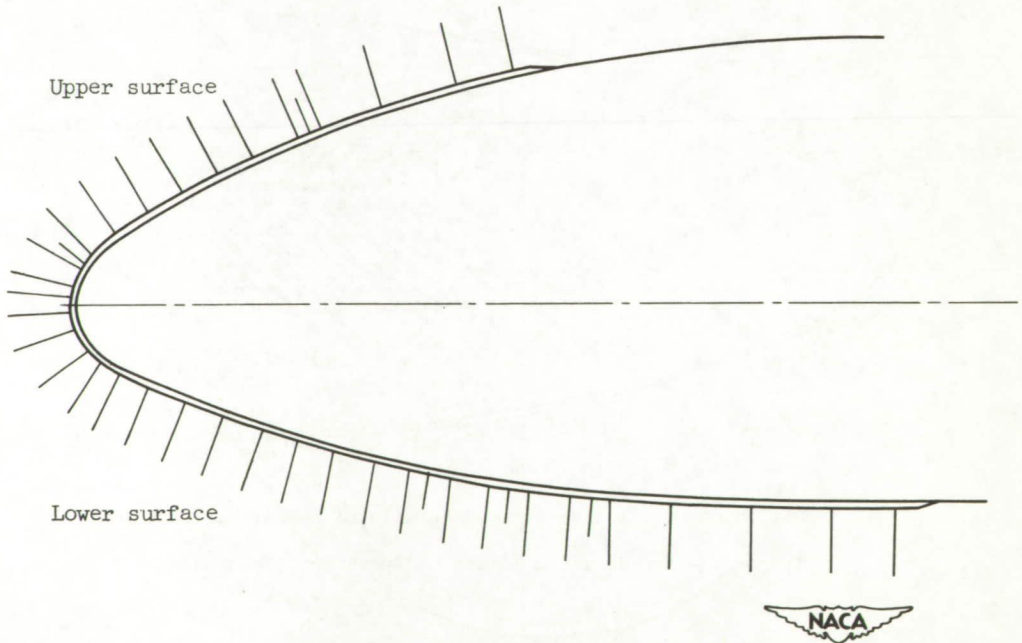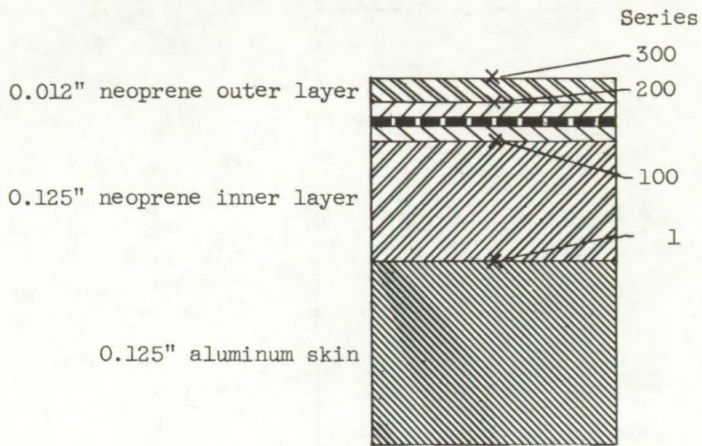
Figure 3. - Location of heater thermocouples.
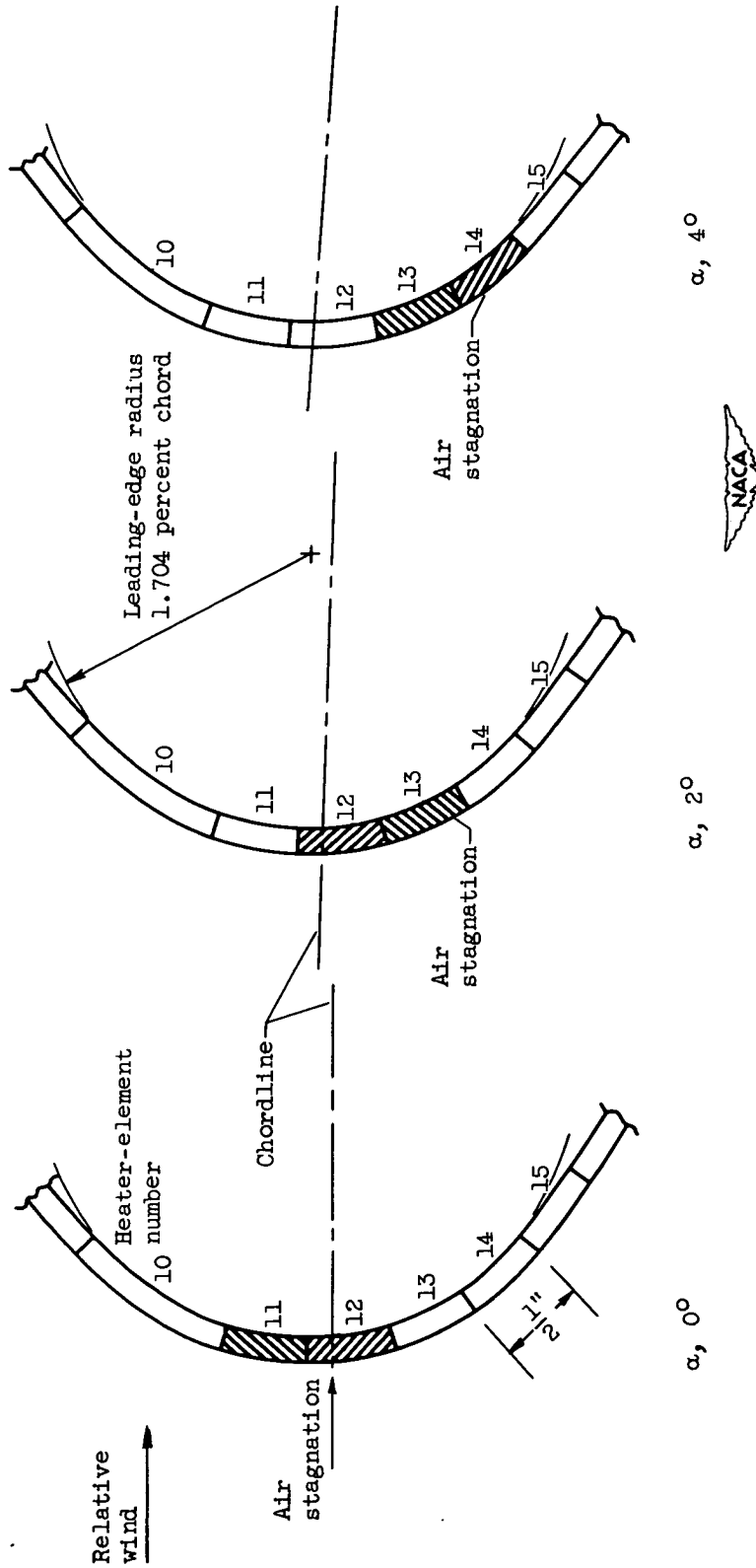
Figure 4. - Location of parting strips at various angles of attack. Shaded areas indicate continuously heated elements.
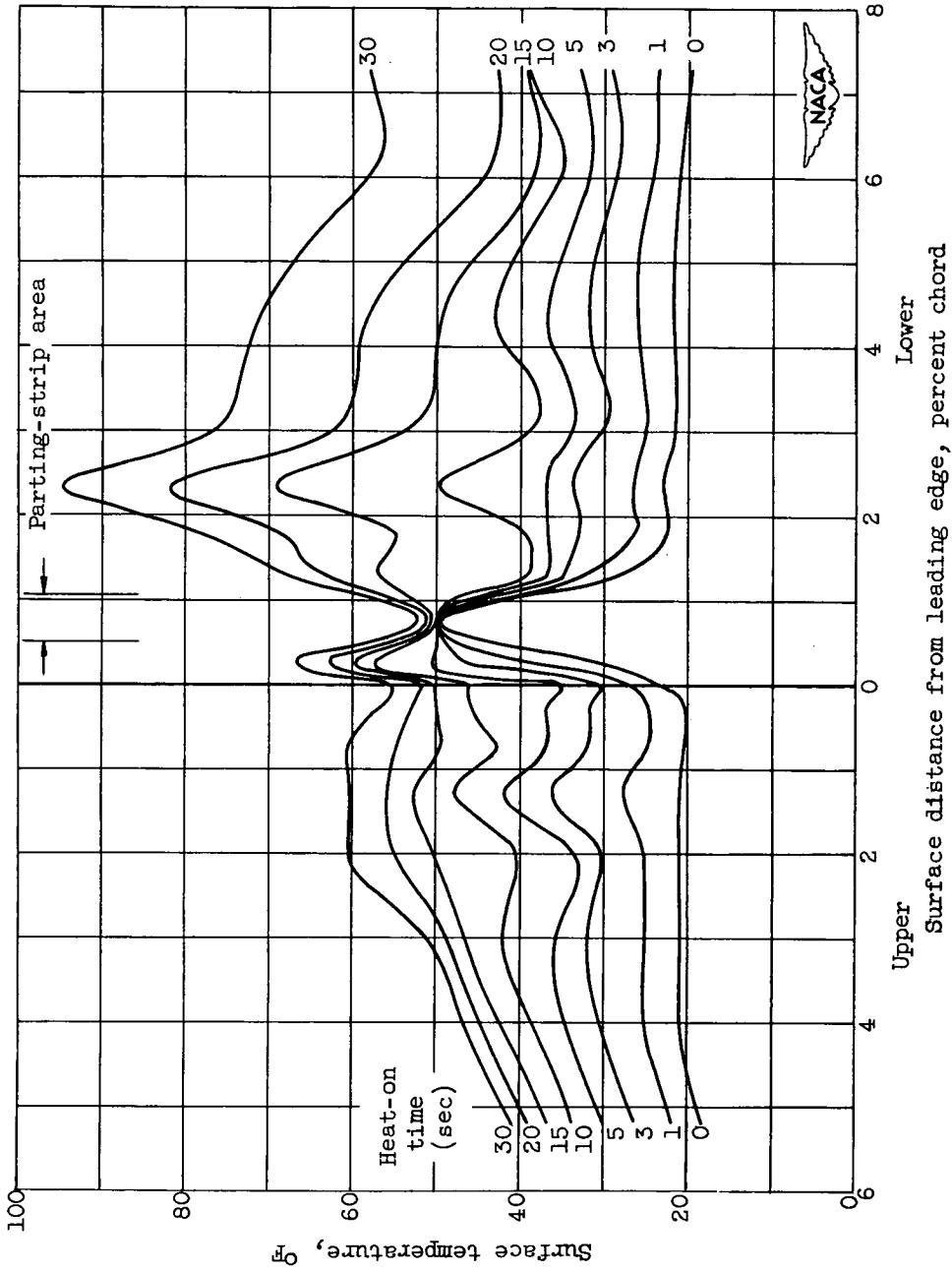
Figure 5. - Variation of surface temperature distribution with heat-on time. Airspeed, 175 miles per hour; angle of attack, 4°; stagnation wet datum temperature, 19° F; liquid-water content, 0.65 gram per cubic meter; heat-on period, 30 seconds.

(a) With parting strip.
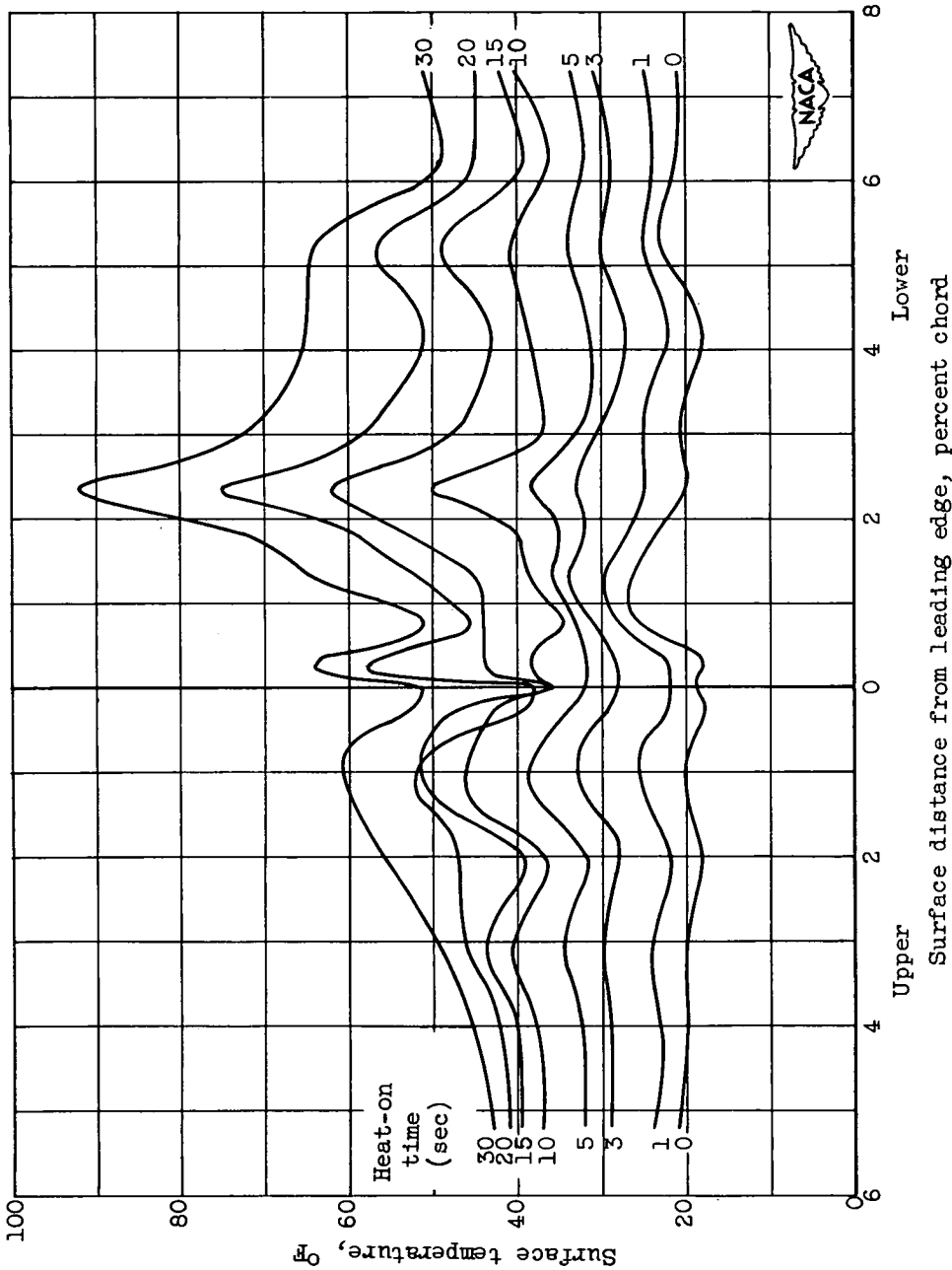
(b) All-cycled condition.

Figure 5. - Concluded. Variation of surface temperature distribution with heat-on time. Airspeed, 175 miles per hour; angle of attack, 4°; stagnation wet datum temperature, 19° F; liquid-water content, 0.65 gram per cubic meter; heat-on period, 30 seconds.
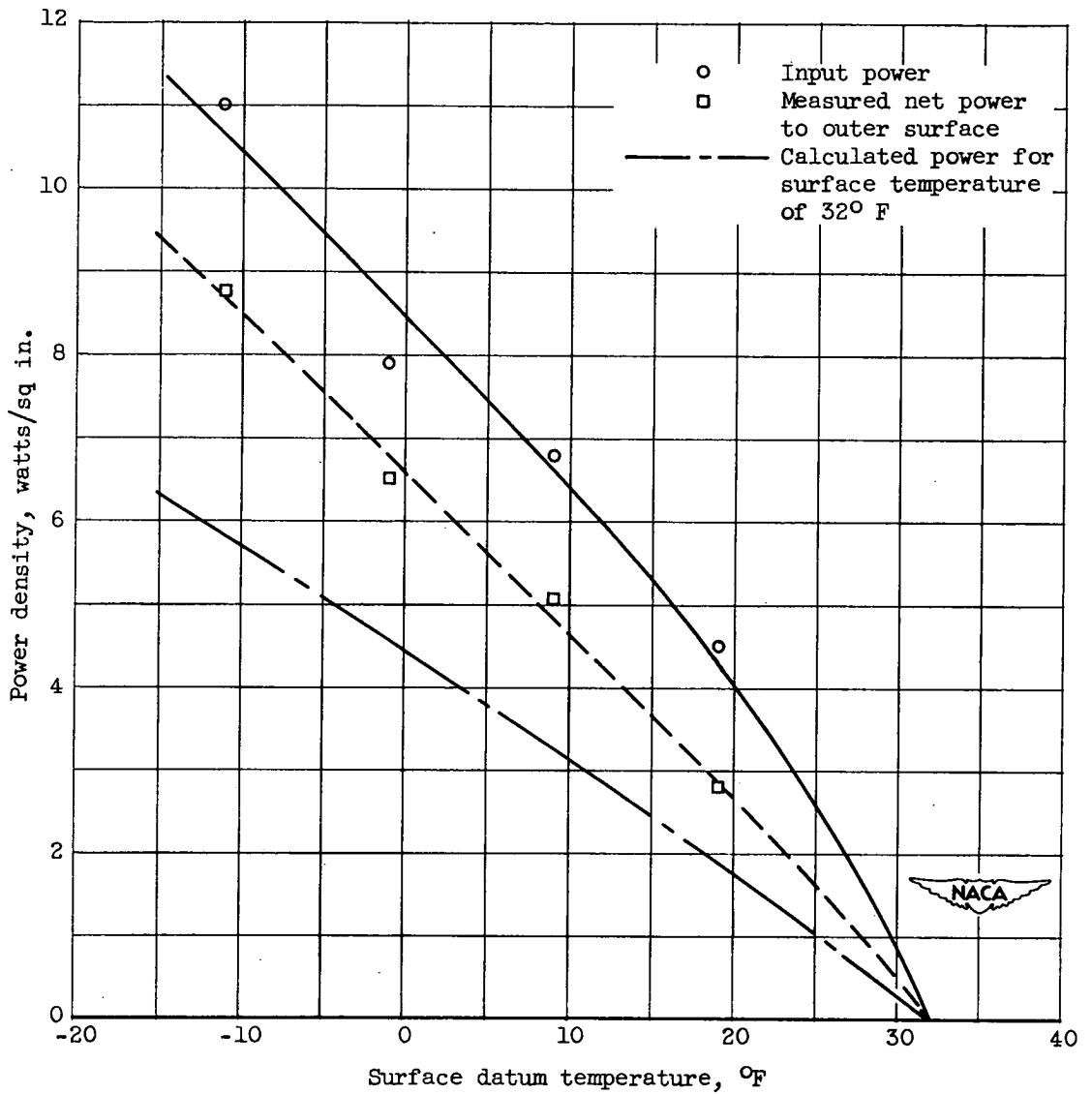
Figure 6. - Power requirements for parting strip. Airspeed, 175 miles
per hour; angle of attack, 2°.
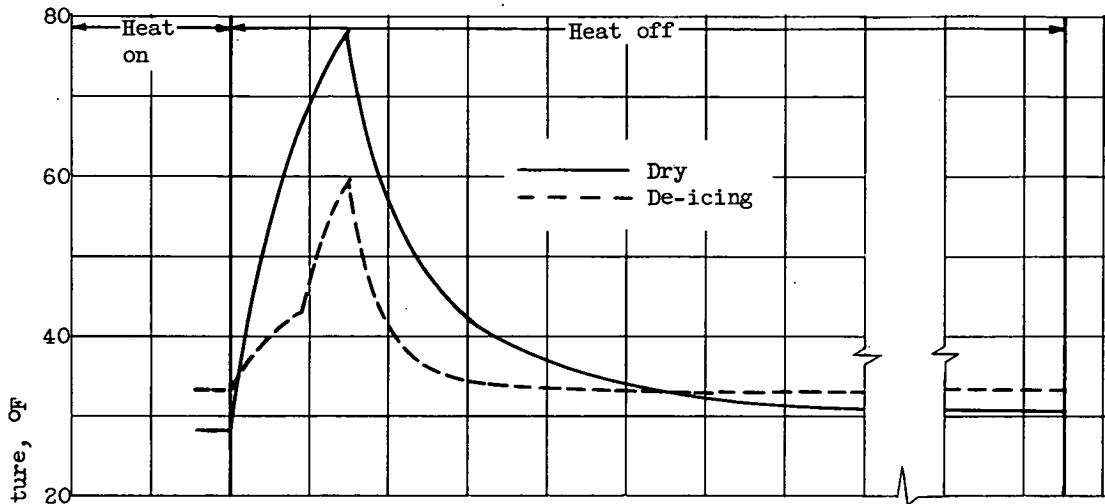
(a) Lower surface; S/C, 1.3 percent.
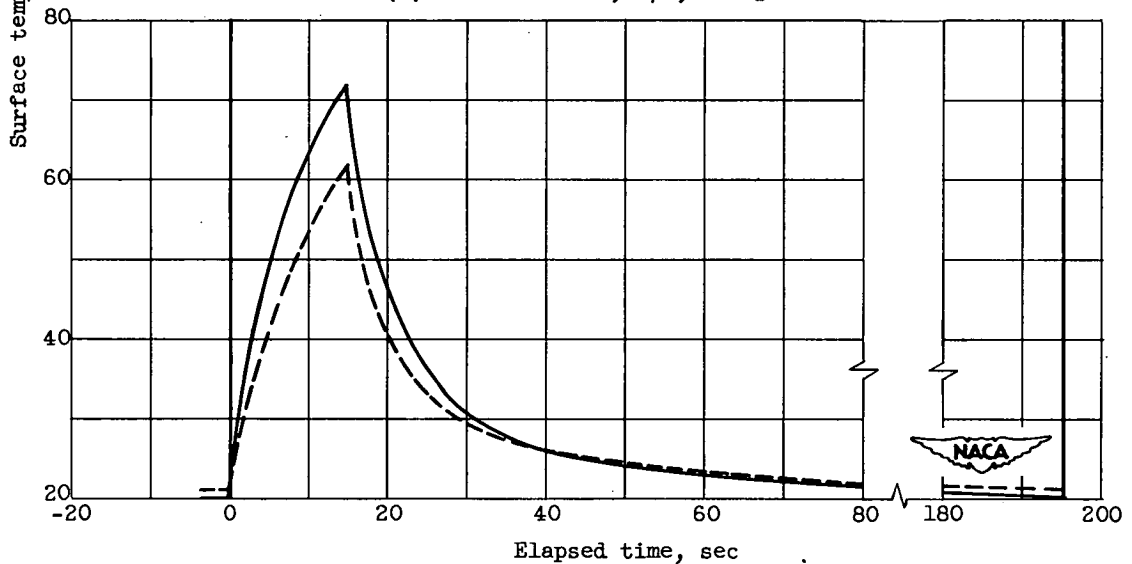
(b) Upper surface; S/C, 0.78 percent.

Figure 7. - Comparison of measured surface temperatures in dry air and during
   de-icing. Airspeed, 175 miles per hour; angle of attack, 4°; stagnation
   wet datum temperature, 19° F.
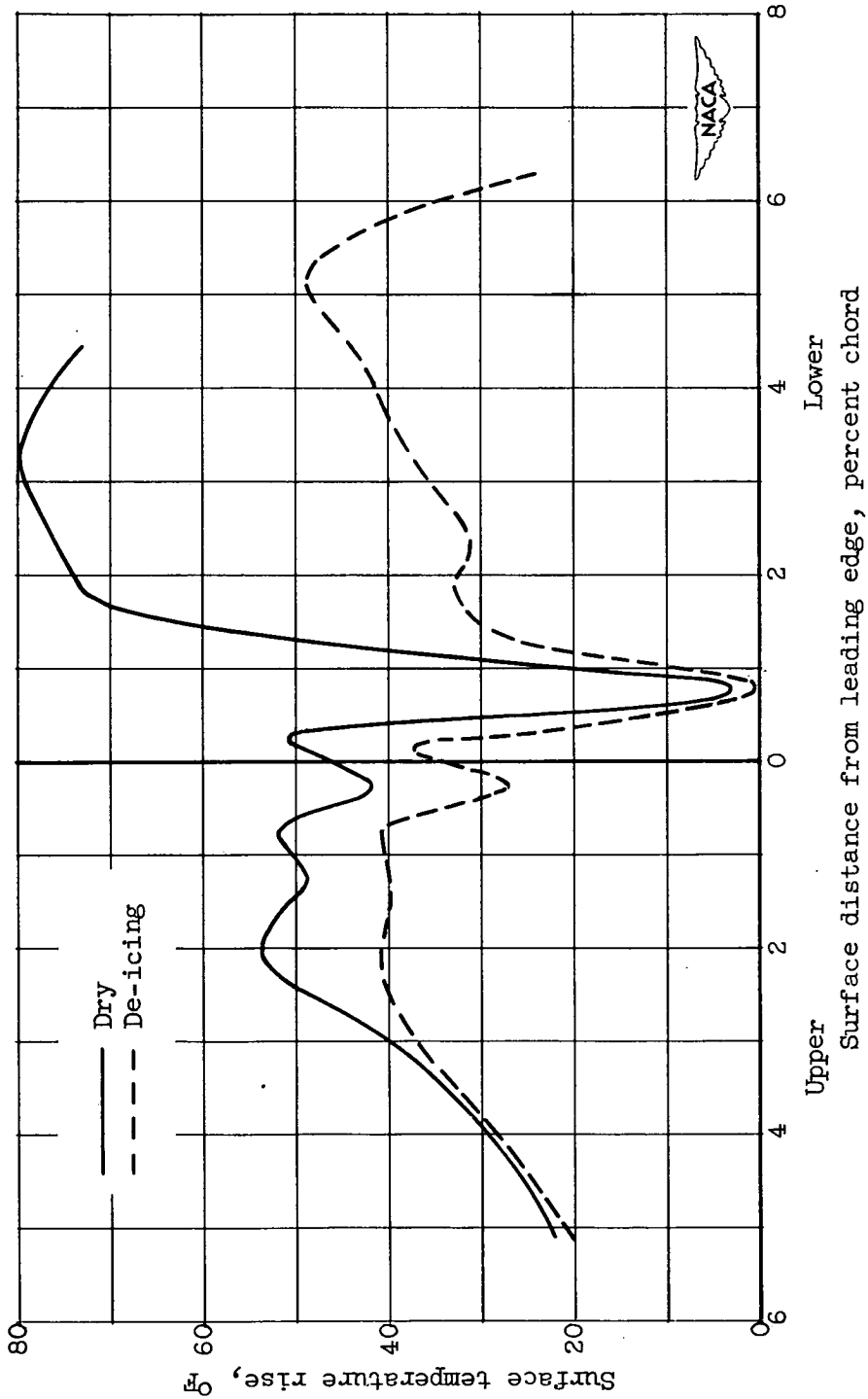
Figure 8. - Comparison of measured surface temperature rise at end of heat-on period in dry air and during cyclic de-icing. Airspeed, 175 miles per hour; angle of attack, 4°; stagnation wet datum temperature, 19° F.
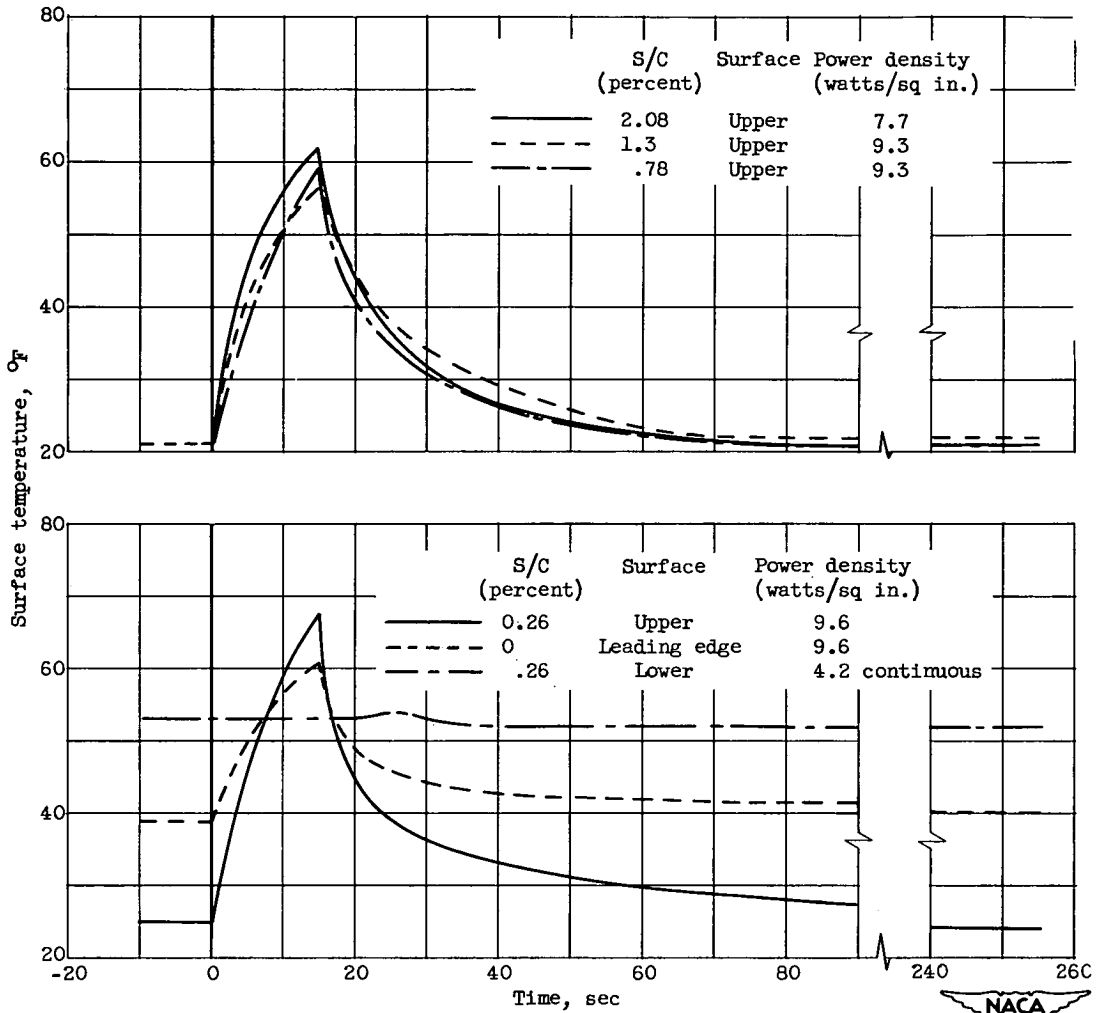
Figure 9. - Variation of surface temperature during cyclic de-icing. Airspeed, 175 miles per hour; angle of attack, 2°; surface datum temperature, 19° F; liquid-water content, 0.65 gram per cubic meter; heat-on period, 15 seconds; heat-off period, 4 minutes.
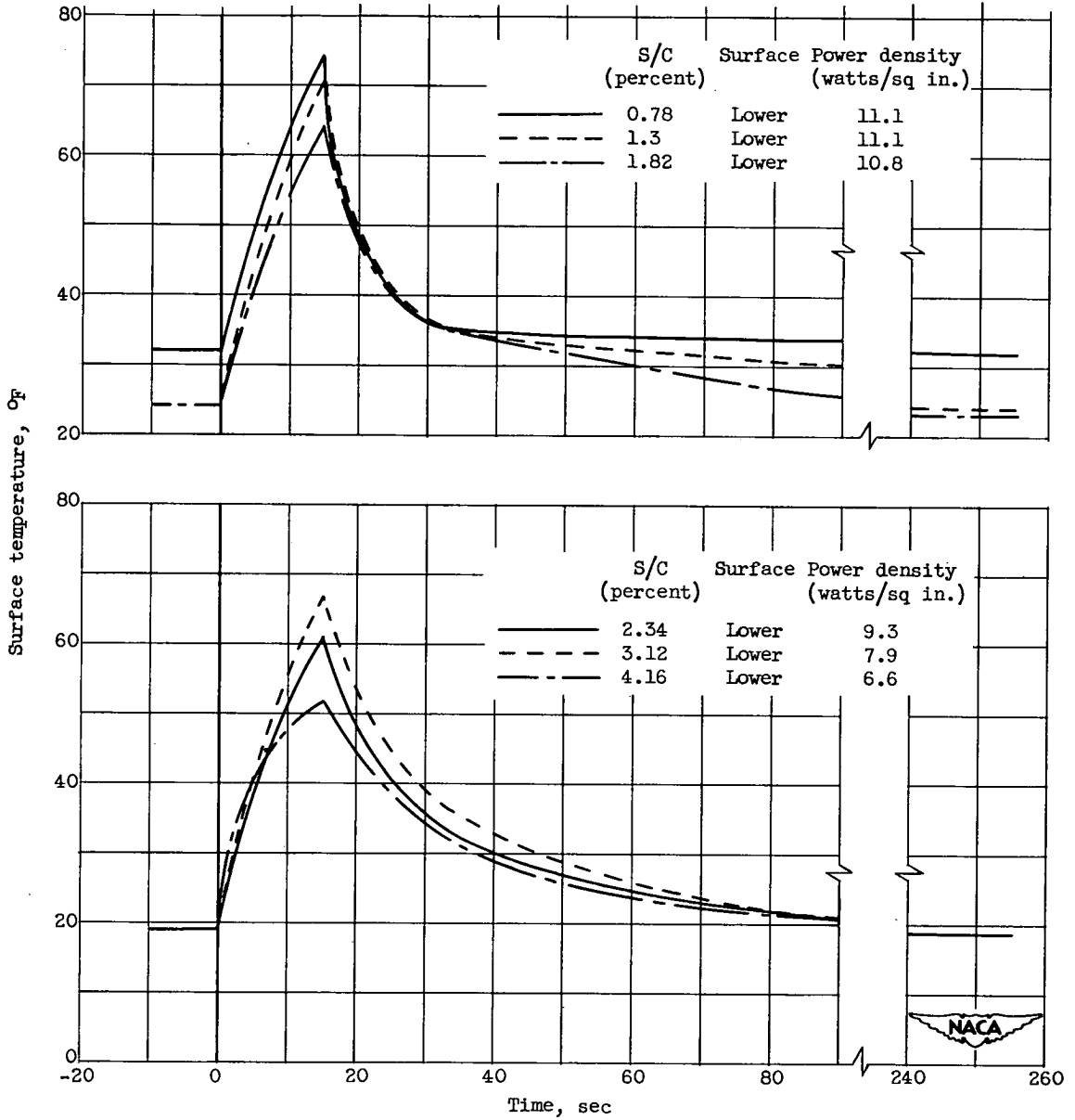
Figure 9. - Concluded. Variation of surface temperature during cyclic de-icing. Airspeed, 175 miles per hour; angle of attack, 2°; surface datum temperature, 19° F; liquid-water content, 0.65 gram per cubic meter; heat-on period, 15 seconds; heat-off period, 4 minutes.
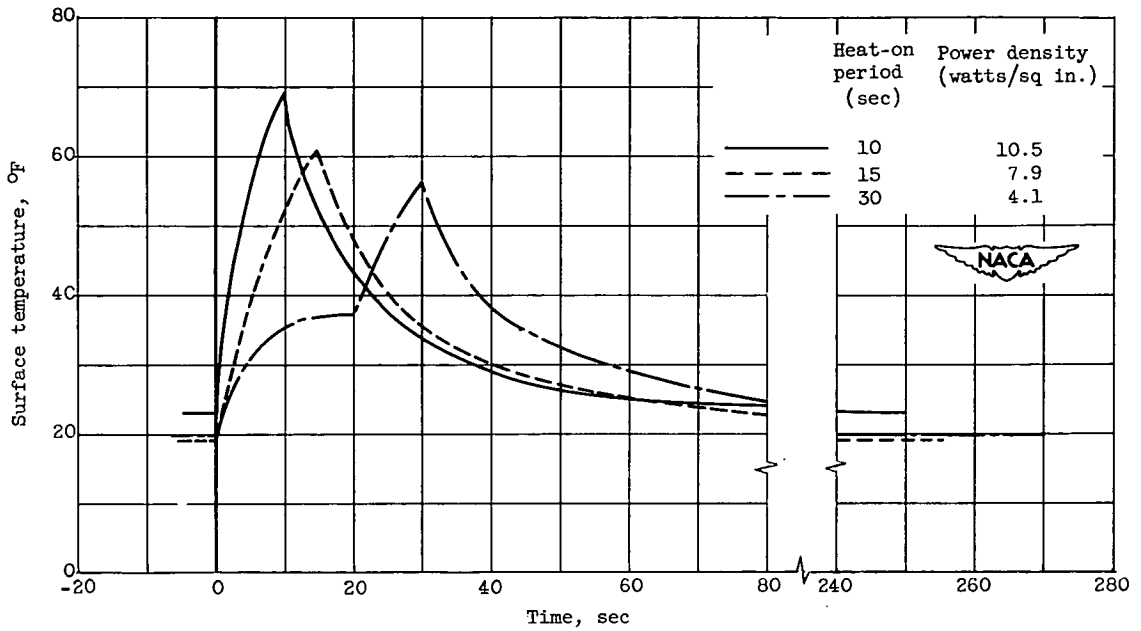
Figure 10. - Variation of surface temperature at 2.34 percent chord, lower surface, for three heat-on periods. Airspeed, 175 miles per hour; datum temperature, 19° F; liquid-water content, 0.65 gram per cubic meter; heat-off period, 4 minutes; angle of attack, 2°.
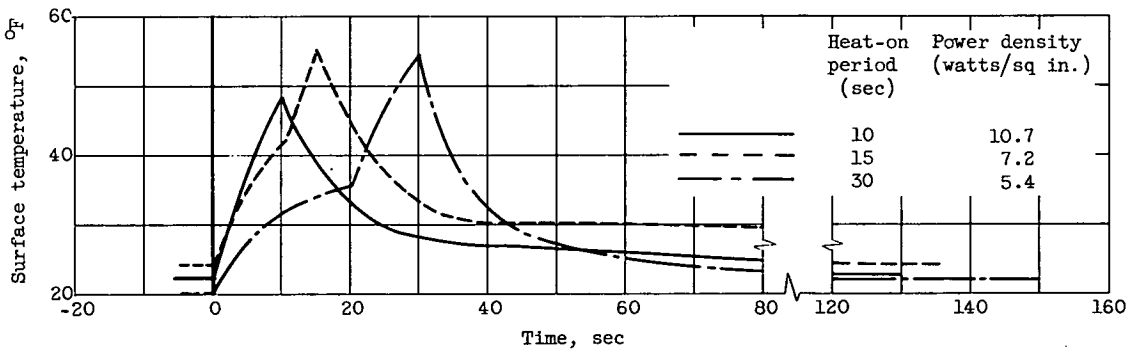
Figure 11. - Variation of surface temperature at 2.34 percent chord, lower surface, for three heat-on periods. Airspeed, 175 miles per hour; datum temperature, 19° F; liquid-water content, 1.0 gram per cubic meter; heat-off period, 2 minutes; angle of attack, 2°.
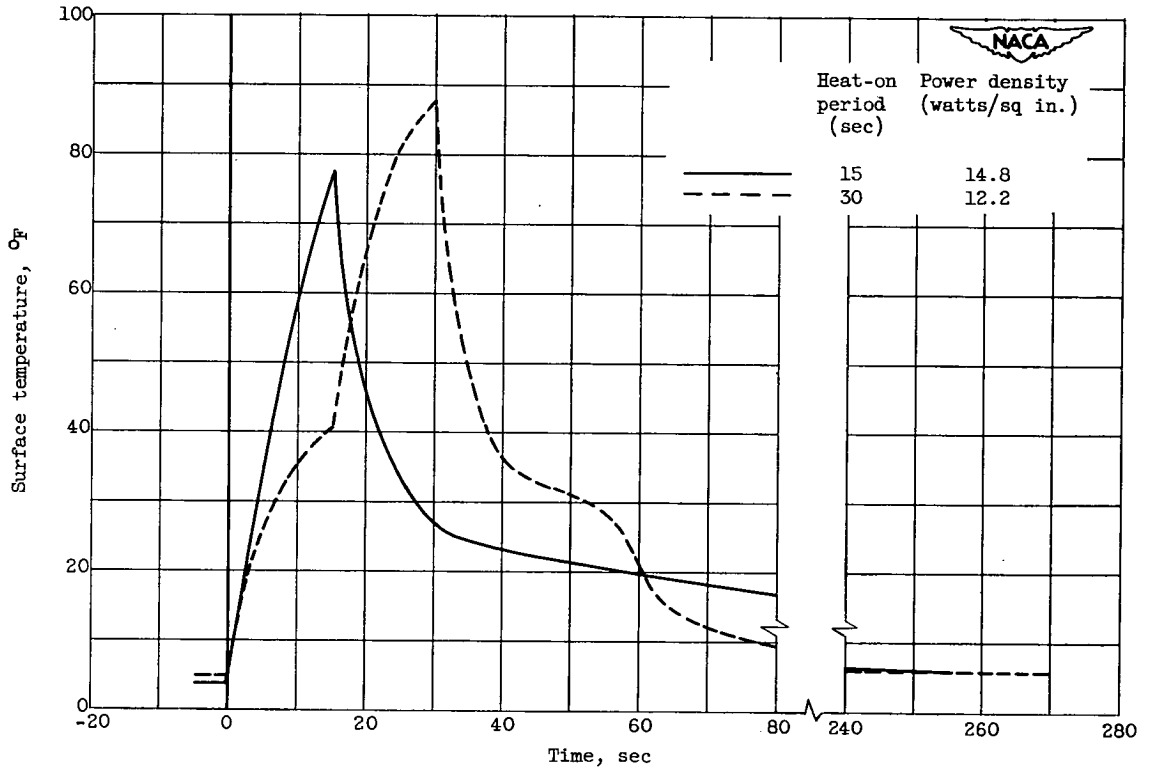
Figure 12. - Variation of surface temperature at 2.34 percent chord, lower surface, for two heat-on periods. Airspeed, 175 miles per hour; datum temperature, -1° F; liquid-water content, 1.0 gram per cubic meter; heat-off period, 4 minutes.
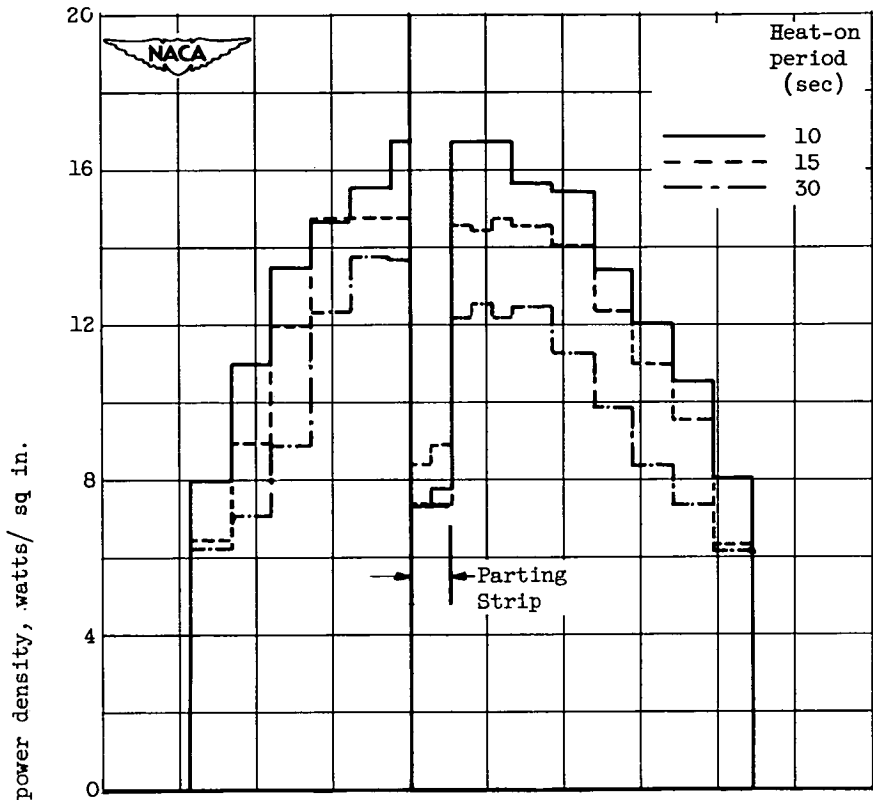
(a) Datum temperature, -1° F.
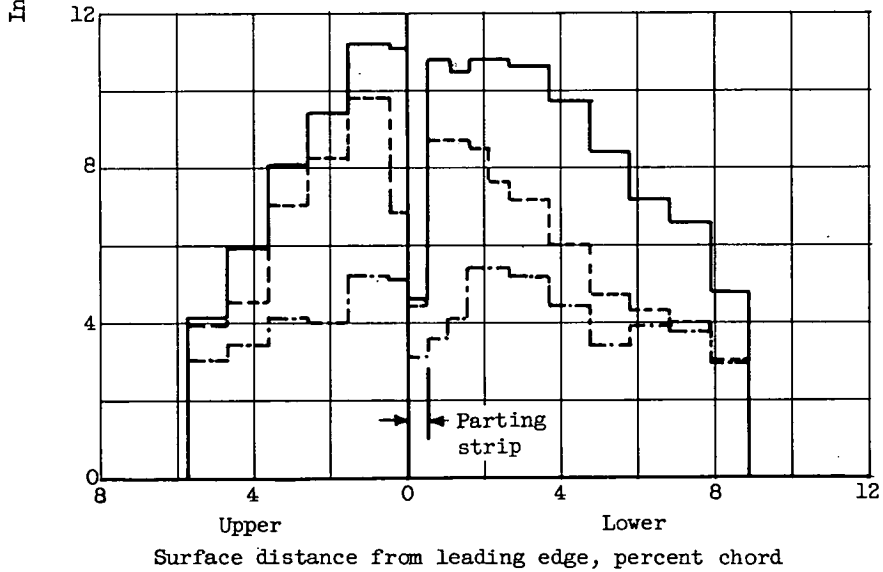
(b) Datum temperature, 19° F.

Figure 13. - Distribution of input power for three heat-on
    periods and two datum temperatures. Airspeed, 175 miles
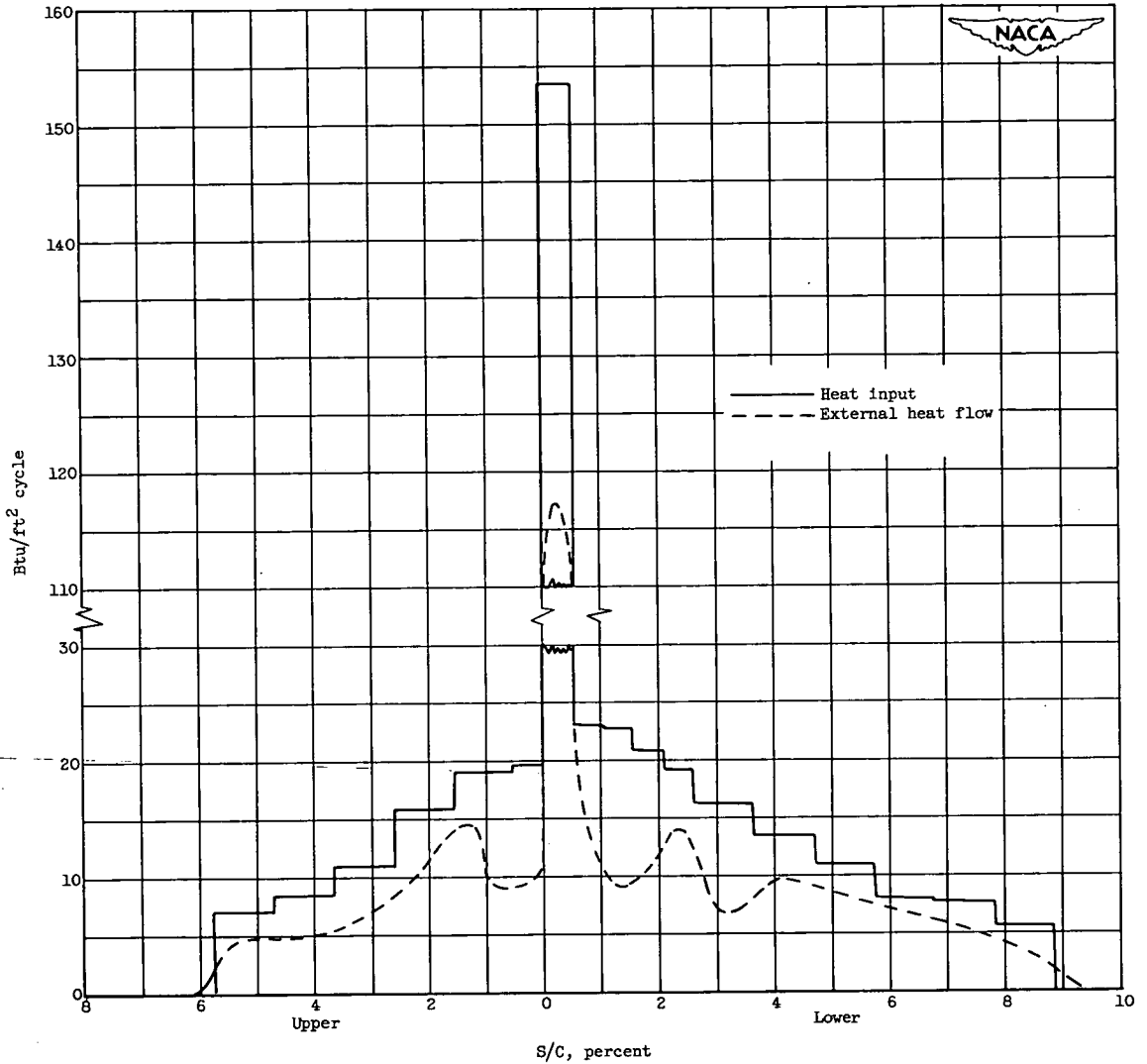   per hour; angle of attack, 2°; liquid-water content, 1.0
    gram per cubic meter; heat-off period, 2 minutes.
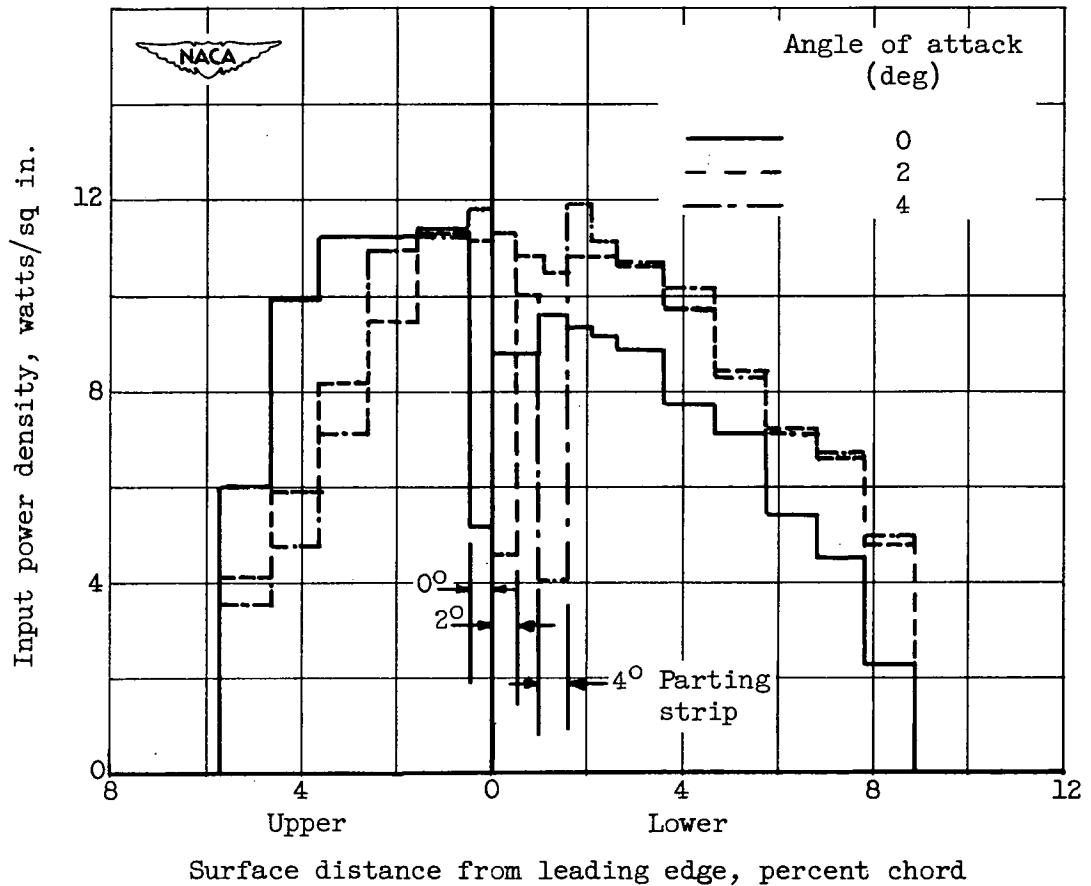
Figure 14. - Distribution of input power for three angles of attack. Airspeed, 175 miles per hour; datum temperature, 19° F; heat-on period, 10 seconds; heat-off period, 2 minutes.

	Heat-on period (sec)	Liquid-water content (gram/cu m)	Heat-off period (sec)
○	10	1.0	240
♂	10	.65	240
●	10	1.0	120
□	15	1.0	240
◪	15	.65	240
◼	15	.65	120
◇	30	1.0	240
◈	30	.65	240
◆	30	1.0	120
◆	30	.65	120
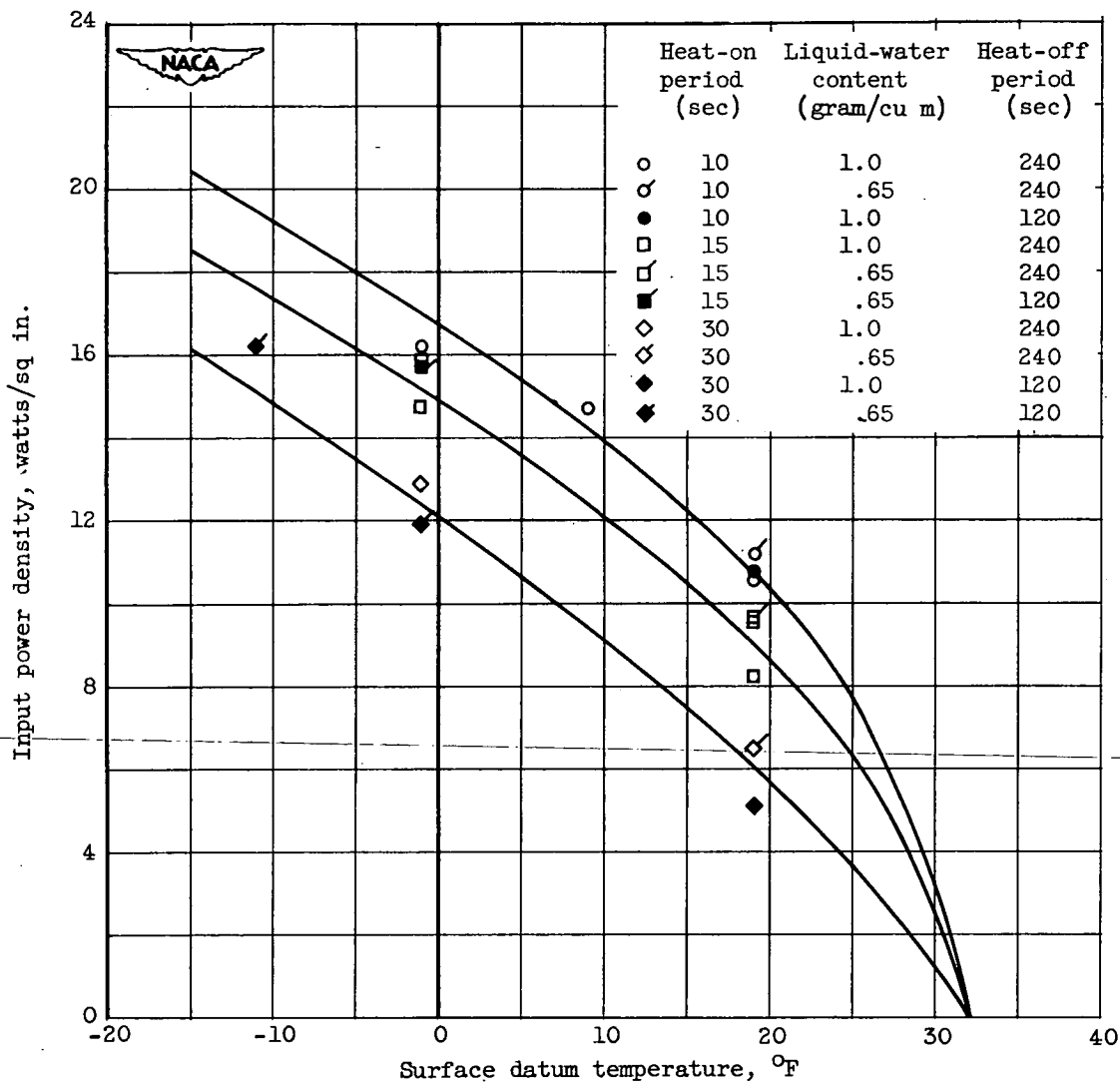
Figure 15. - Variation of cycled power density with datum temperature. Airspeed, 175 miles per hour; angle of attack, 2°. Power densities are average of input power to heaters 10 to 17.
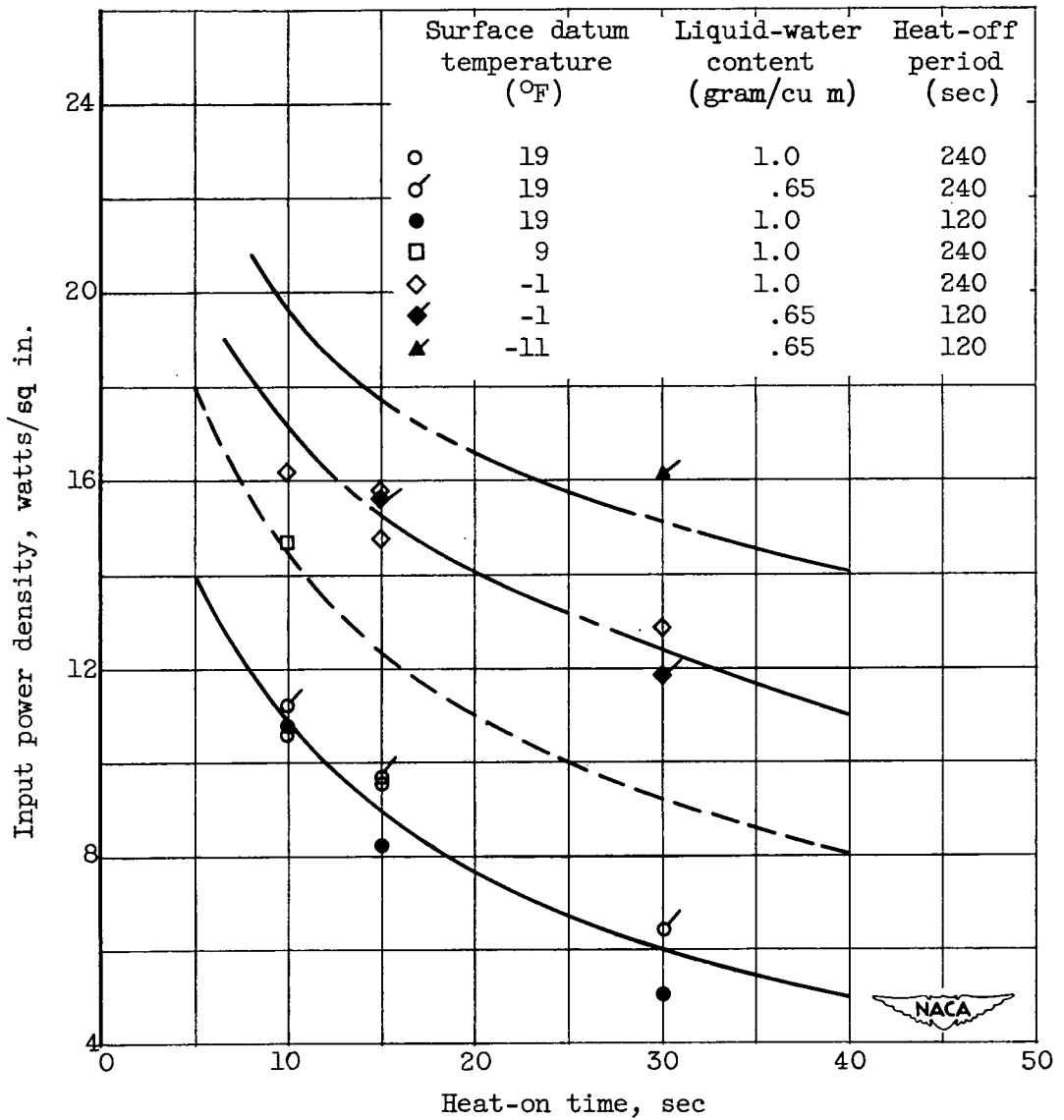
Figure 16. - Variation of input cycled power density with heat-on
time for various heat-off periods and datum temperatures.
Airspeed, 175 miles per hour; angle of attack, 2°. Power
densities are average of power to heaters 10 to 17.
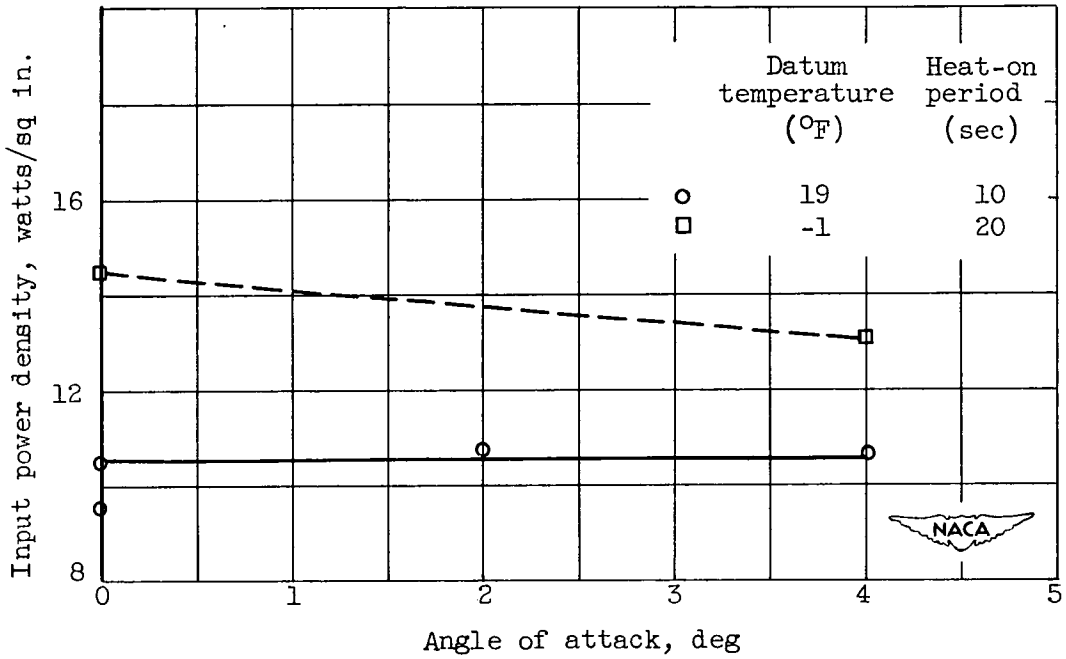
Figure 17. - Variation of input cycled power density with angle
   of attack. Airspeed, 175 miles per hour; heat-off period,
   4 minutes. Power densities are average of power to elements
   10 to 17.
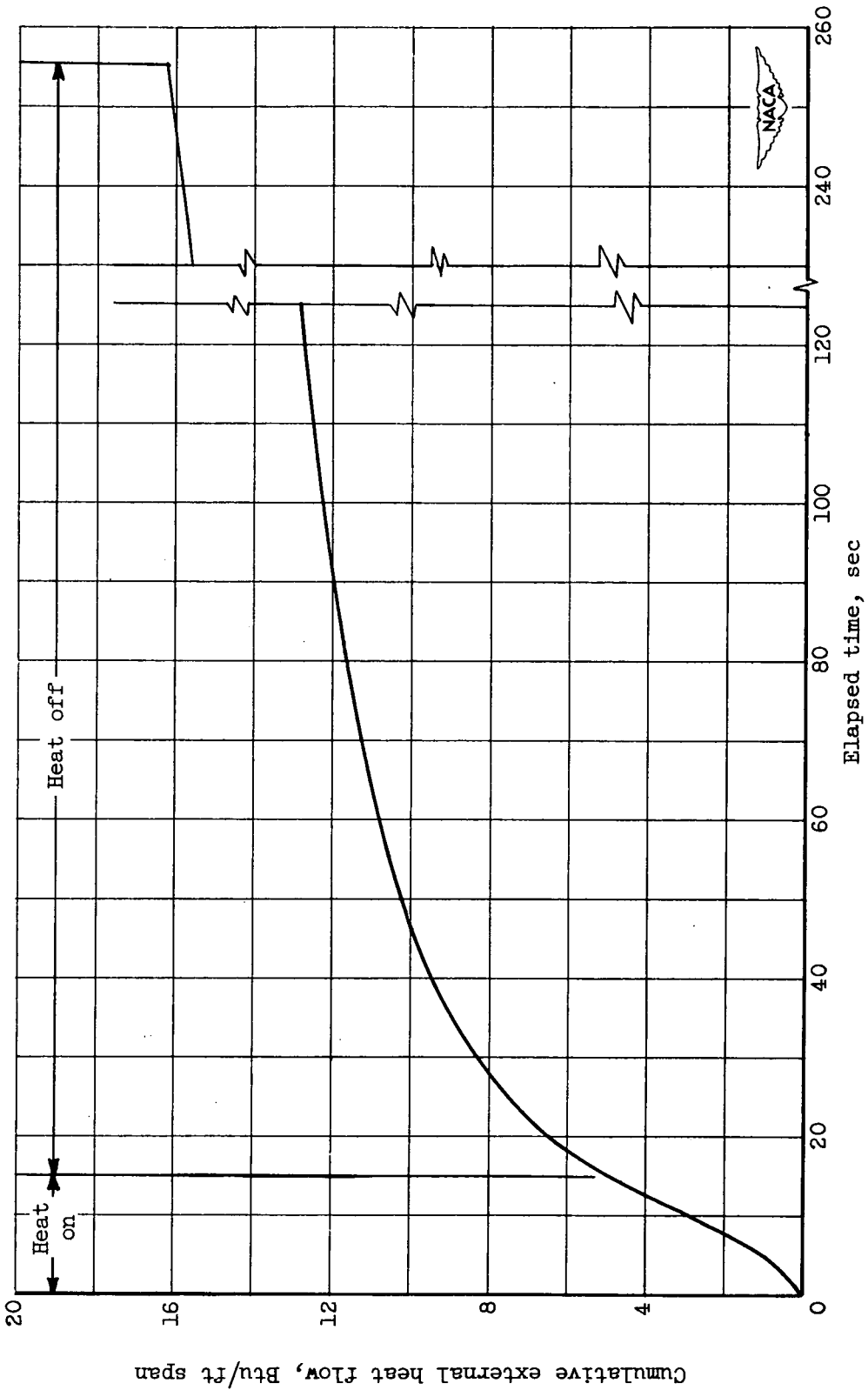
Figure 18. - External heat flow during cyclic de-icing. Airspeed, 175 miles per hour; datum temperature, 19° F; liquid-water content, 0.65 gram per cubic meter; heat-on period, 15 seconds; heat-off period, 4 minutes.

Figure 19. - Comparison of external heat flow with total heat input for one complete cycle. Airspeed, 175 miles per hour; angle of attack, 2°; datum temperature, 19° F; liquid-water content, 0.65 gram per cubic meter; heat-on period, 15 seconds; heat-off period, 4 minutes.

(a)   External heat flow.
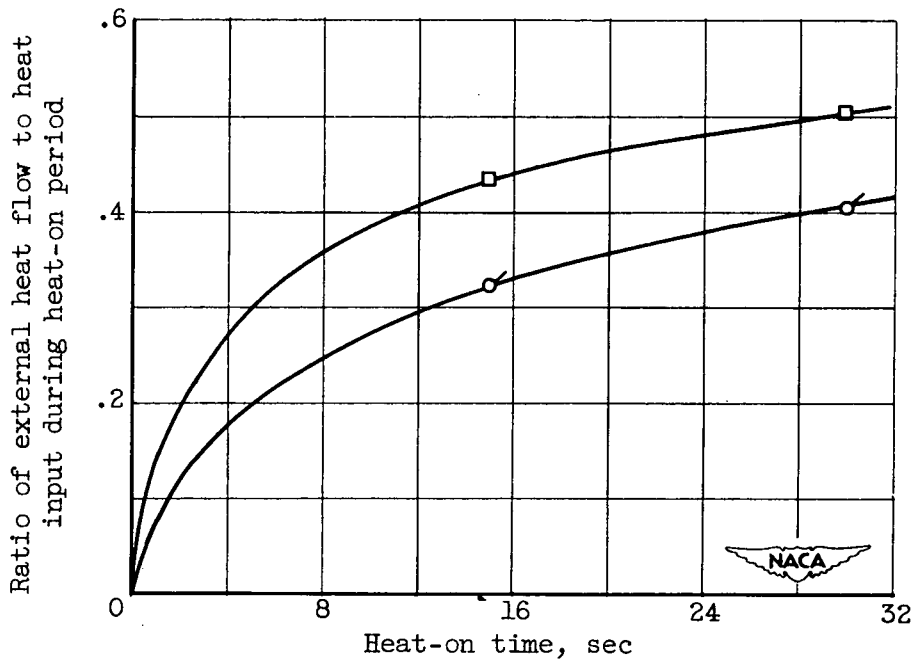
(b)   Ratio of external heat flow to heat input.

Figure 20. - Variation of external heat flow from
heater during heat-on period for various heat-on
and heat-off times and two liquid-water contents.
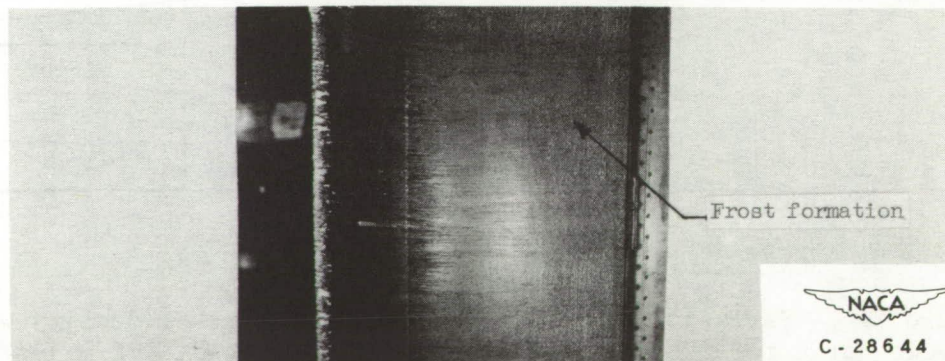Airspeed, 175 miles per hour; angle of attack, 2°;
datum temperature, 19° F.
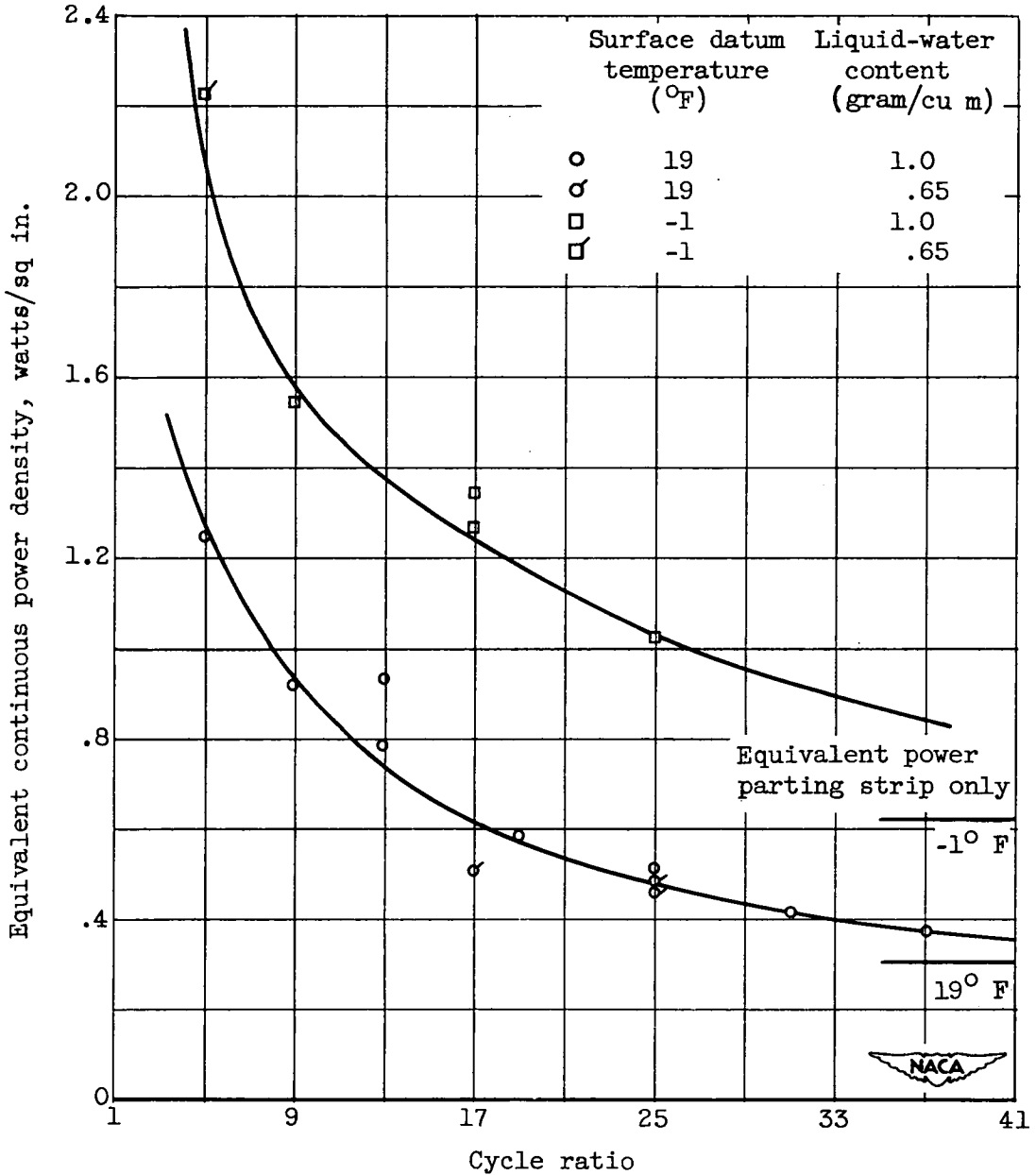
Figure 21. - Variation of equivalent continuous power density with cycle ratio for two datum temperatures. Airspeed, 175 miles per hour; angle of attack, 2°.
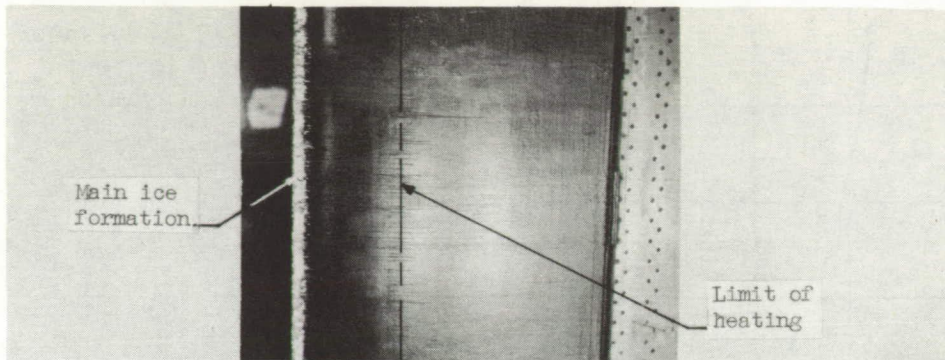
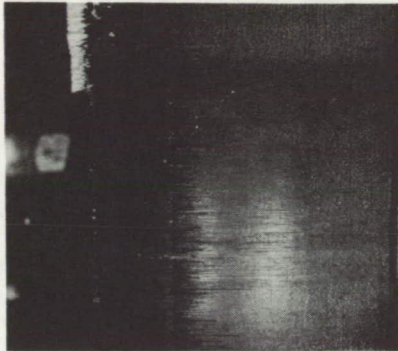(a) 4 minute icing, second cycle.   Total icing time, 8 minutes, 20 seconds.
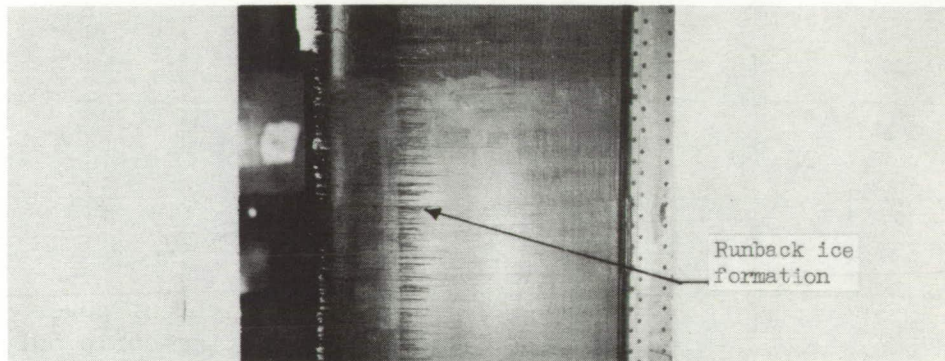
(b) After 20 second heat-on period, third cycle.   Total icing time, 13 minutes.
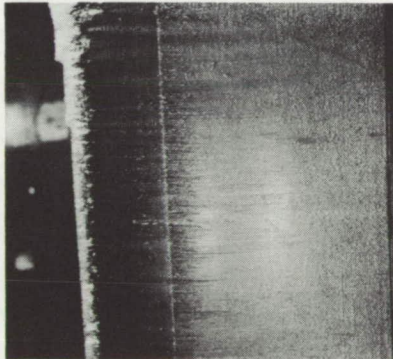

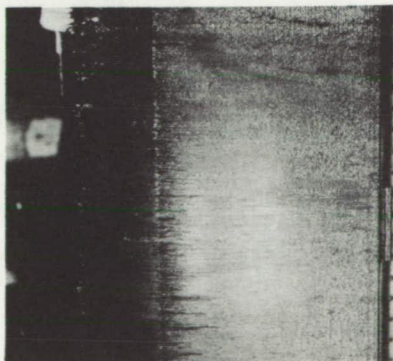(c) 4 minute icing, ninth cycle.   Total icing time, 38 minutes, 40 seconds.

Figure 22. - Growth of runback formation on lower surface of heater during cyclic de-icing.
Airspeed, 175 miles per hour; datum temperature, -1° F; angle of attack, 0°; liquid-
water content, 1.0 gram per cubic meter; heat-on period, 20 seconds; heat-off period,
4 minutes.

(d) After 20 second heat-on period, tenth cycle.   Total icing time, 43 minutes, 20 seconds.

(e) 4 minute icing, twelfth cycle.   Total icing time, 51 minutes, 40 seconds.

(f) After 20 second heat-on period, thirteenth cycle.   Total icing time,
56 minutes, 20 seconds.

Figure 22. - Concluded. Growth of runback formation on lower surface of heater during
cyclic de-icing. Airspeed, 175 miles per hour; datum temperature, -1° F; angle of
attack, 0°; liquid-water content, 1.0 gram per cubic meter; heat-on period, 20 seconds;
heat-off period, 4 minutes.